



Published in final edited form as:

*Neuroimage*. 2013 January 15; 65: 176–193. doi:10.1016/j.neuroimage.2012.10.008.

## Variation in longitudinal trajectories of regional brain volumes of healthy men and women (ages 10 to 85 years) measured with atlas-based parcellation of MRI

Adolf Pfefferbaum<sup>1,2</sup>, Torsten Rohlfing<sup>1</sup>, Margaret J. Rosenbloom<sup>1,2</sup>, Weiwei Chu<sup>1</sup>, Ian M. Colrain<sup>3</sup>, and Edith V. Sullivan<sup>2</sup>

<sup>1</sup>Neuroscience Program, SRI International, Menlo Park, CA

<sup>2</sup>Department of Psychiatry & Behavioral Sciences, Stanford University School of Medicine, Stanford, CA

<sup>3</sup>Human Sleep Laboratory, SRI International, Menlo Park, CA

### Abstract

Numerous cross-sectional MRI studies have characterized age-related differences in regional brain volumes that differ with structure and tissue type. The extent to which cross-sectional assumptions about change are accurate depictions of actual longitudinal measurement remains controversial. Even longitudinal studies can be limited by the age range of participants, sex distribution of the samples, and scan intervals. To address these issues, we calculated trajectories of regional brain volume changes from T1-weighted (SPGR) MRI data, quantified with our automated, unsupervised SRI24 atlas-based registration and parcellation method. Longitudinal MRIs were acquired at 3T in 17 boys and 12 girls, age 10 to 14 years, and 41 men and 41 women, age 20 to 85 years at first scan. Application of a regression-based correction factor permitted merging of data acquired at 3T field strength with data acquired at 1.5T from additional subjects, thereby expanding the sample to a total of 55 men and 67 women, ages 20 to 85 years at first scan. Adjustment for individual supratentorial intracranial volume removed regional volume differences between men and women due to sex-related differences in head size. Individual trajectories were computed from data collected on 2 to 6 MRIs at a single field strength over a ~1 to 8 year interval. Using the linear mixed-effects model, the pattern of trajectories over age indicated: rises in ventricular and Sylvian fissure volumes, with older individuals showing faster increases than younger ones; declines in selective cortical volumes with faster tissue shrinkage in older than younger individuals; little effect of aging on volume of the corpus callosum; more rapid expansion of CSF-filled spaces in men than women after age 60 years; and evidence for continued growth in central white matter through early adulthood with accelerated decline in senescence greater in men than women.

---

© 2012 Elsevier Inc. All rights reserved.

Correspondence: Edith, V., Sullivan, Ph.D, Department of Psychiatry and Behavioral Sciences, Stanford University School of Medicine (MC5723), 401 Quarry Road, Stanford, CA 94305-5723, phone: (650) 859-2880, FAX: (650) 859-2743, edie@stanford.edu.

#### Statement on conflict of interest

No author of this manuscript has any conflicts of interest with this work, either financial or otherwise.

**Publisher's Disclaimer:** This is a PDF file of an unedited manuscript that has been accepted for publication. As a service to our customers we are providing this early version of the manuscript. The manuscript will undergo copyediting, typesetting, and review of the resulting proof before it is published in its final citable form. Please note that during the production process errors may be discovered which could affect the content, and all legal disclaimers that apply to the journal pertain.

## Keywords

longitudinal; MRI; brain; field strength; atlas-based parcellation; image registration; SRI24 atlas

---

## Introduction

Numerous cross-sectional MRI studies have characterized age-related differences in regional brain volumes that differ with structure and tissue type. In general, these brain imaging studies are consistent in reporting larger cerebrospinal fluid (CSF) filled volumes (ventricles and sulci), smaller brain tissue volumes, more prominent in cortical and allocortical gray matter than in centrum semiovale or corpus callosum white matter, and thinner cortices (e.g., Blatter et al., 1995; Courchesne et al., 2000; Good et al., 2001; Jernigan et al., 2001; Pfefferbaum et al., 1994; Raz et al., 2004a; Sowell et al., 2007; Sullivan et al., 2004; Walhovd et al., 2011); (reviewed by Raz and Kennedy, 2009; but see Burgmans et al., 2009). Age-related shrinkage of selective subcortical structures is controversial (e.g., Jack et al., 2000; Jernigan et al., 2001; Luft et al., 1999; Raz et al., 2003; Sullivan et al., 2005; Sullivan et al., 2004). One of the largest cross-sectional samples analyzed 1143 healthy men and women, age 18 to 94 years, from seven imaging centers and measured cortical thickness and regional volumes acquired on different 1.5T MRI systems and measured with a single method (FreeSurfer) (Fjell et al., 2009b). This analysis revealed small but significant sex differences in white matter, CSF, and the pallidum, suggesting more rapid age effects in older men than women; however, caution is required for data based on the pallidum measure because it was the least reliable of those used (Pfefferbaum et al., 2012). The extent to which cross-sectional assumptions about change reflect true longitudinal measurement, however, remains controversial (cf., Lindenberger et al., 2011; Rabbitt, 2011; Raz and Lindenberger, 2011; Salthouse, 2011). Statistical modeling has identified notable shortcomings in making longitudinal inferences about change from cross-sectional data, even in instances where cross-sectional measures correlate well with longitudinal change (e.g., Lindenberger et al., 2011).

Longitudinal studies are better suited to address conflicts emerging from cross-sectional investigation (cf., Lindenberger et al., 2011; Weiner et al., 2012). Such studies report ventricular enlargement or brain tissue volume decline detectable over one year (Adalsteinsson et al., 2000; Fjell et al., 2009a) to several years (e.g., Cook et al., 2004; Marcus et al., 2010; Pfefferbaum et al., 1998; Raji et al., 2009; Raz et al., 2005; Resnick et al., 2003; Rusinek et al., 2003; Scahill et al., 2003; Sullivan et al., 2010; Sullivan et al., 2004; Taki et al., 2011b; Tang et al., 2001), with the longest follow-up to date being 10 years (Driscoll et al., 2009). Brain regional volumes commonly identified as exhibiting the greatest aging effects are prefrontal cortex, medial temporal lobe structures, and lateral ventricles. As with cross-sectional studies, these longitudinal studies provide only inconsistent evidence for sex differences in rates of change. The series of analyses by Raz and colleagues on trajectories of local volume decline in striatum (Raz et al., 2003), entorhinal cortex, hippocampus (Raz et al., 2004b; Rodrigue and Raz, 2004), and cerebellum (Raz et al., 2005) culminated in an analysis comparing rates of change in these and other brain structures, examined three times on a 1.5T MRI system over a 30-month interval in 40 participants, age 49 to 85 years, and subjected to manual delineation of target brain structures (Raz et al., 2010). Adjusted for variation in intracranial volume, areas especially vulnerable to aging were the lateral prefrontal cortex, prefrontal white matter, hippocampus, putamen, and cerebellar hemispheres; the least affected were the primary visual cortex, corpus callosum, and ventral pons; the only sex difference reported was for the pons, where women showed greater shrinkage than men. Another study of 3 measurements over 4 years in 92 men and women, age 59 to 85 years, revealed widespread white matter volume decline

with local gray matter volume decline, which was most prominent in inferior and orbital frontal, inferior parietal, insular and cingulate cortices, and ventricular enlargement with little evidence for sex differences in rates of change (Resnick et al., 2003). A 6-year longitudinal study in 381 community-dwelling men and women, age 28 to 89 years, reported greater annual declines in gray matter-to-intracranial volume ratios in older men and women relative to younger women (Taki et al., 2011a).

Cross-sectional developmental studies focused on adolescence have revealed a curvilinear function of cortical gray matter with an increase from birth to about 10 years of age followed by a continuous decline through adulthood to old age (Blanton et al., 2001; Carne et al., 2006; Courchesne et al., 2000; Giedd et al., 1996; for reviews Giedd et al., 2010; Gogtay et al., 2004; e.g., Jernigan et al., 2001; Lange et al., 1997; Lu et al., 2007; Pfefferbaum et al., 1994; Raz and Rodrigue, 2006; Reiss et al., 1996; Sowell et al., 2007; Sowell et al., 2002; Stiles and Jernigan, 2010; Tisserand et al., 2002). Longitudinal studies are consistent with this depiction of regional brain volumetric change when regional brain volumes obtained over time are expressed as individual trajectories (Giedd et al., 1996; Raznahan et al., 2011b; Shaw et al., 2008). These analyses characterized heterochronicity in trajectories by brain region and sex (Brain Development Cooperative Group, 2012; Giedd et al., 1999; Lenroot et al., 2007; Raznahan et al., 2011a; Raznahan et al., 2011b; Shaw et al., 2008; Sowell et al., 2004). Brains of boys can be 10% larger than those of girls (Dekaban and Sadowsky, 1978; Goldstein et al., 2001), but growth starts and ends earlier in girls than boys, peaking at 10.5 years in girls compared with 14.5 years in boys and declining thereafter in both (Lenroot et al., 2007).

MRI studies report that the neocortex follows a curvilinear trajectory (Gogtay et al., 2004; Lenroot et al., 2007; Shaw et al., 2008), whereas allocortex and medial temporal structures follow a linear path (Gogtay et al., 2004). Growth is earlier in anterior than posterior cortical regions in both sexes (Shaw et al., 2008). Examination of regional cortical thickness over 2-year intervals revealed continued gray matter thinning of cortical language areas associated with vocabulary scores and probably language development (Sowell et al., 2004). The largest longitudinal study of brain development examined 647 individuals, age 3 to 30 years over approximately 2-year intervals (Raznahan et al., 2011b). Developmental trajectories for regional cortical volumes and surface area analysis revealed curvilinear growth and sexual dimorphism varying by cortical, allocortical, and subcortical tissue structures and developmental stage (also see Raznahan et al., 2010; Raznahan et al., 2011a). Recently, we reported that longitudinal MRI assessment using robust, atlas-based parcellation methods was sufficiently sensitive to identify regional brain changes over a ~6-month interval in boys and girls in early adolescence. Supratentorial and CSF volumes increased, while cortical gray matter volumes declined in anterior (lateral and medial frontal, anterior cingulate, precuneus, and parietal) but not posterior (occipital, calcarine) cortical regions, whereas subcortical structures did not show consistent changes (Sullivan et al., 2011).

Despite power to detect change, longitudinal studies can be limited by the age range of participants recruited for examination. For example, some studies focus on healthy seniors (age 60 years and older), who had served as the comparison group for age-related dementing disorders, or use data taken from publicly available data sources, such as the Alzheimer's Disease Neuroimaging Initiative (ADNI) (e.g., Fjell et al., 2009a; Weiner et al., 2012). Restricting the age range of subjects to the elderly for the purpose of detecting and modeling the effects of aging, however, can potentially introduce a bias in modeling brain structural changes, especially in structures with developmental changes best described by higher-order rather than linear functions. Even longitudinal studies that use restricted age ranges comprise both the obvious longitudinal component, which provides a metric of rate and trajectory of change, and a cross-sectional component, which is related to the age at initial observation.

The cross-sectional component can affect the levels of dependent measures and may exert cohort effects (cf., Schaie and Hofer, 2001). These cross-sectional influences have been characterized as the “selection-maturation interaction” (Nesselroade, 1986), where “selection” refers to the age at study entry and “maturation” refers to the ages over which an individual was studied and the course of maturation over that period. According to Schaie and Hoffer (Schaie and Hofer, 2001), this interaction can be measured and even accounted for by examining multiple, parallel samples. Analysis of simple slopes of the longitudinal component describing change per individual does not fully address the cross-sectional component, which can potentially affect the initial level of trajectories. Thus, we assert that a statistical model incorporating both components should be employed to analyze data collected in the typical mixed longitudinal design.

Most studies of normal aging have been conducted at 1.5T field strength (e.g., Fjell et al., 2009b; Raz et al., 2010; Weiner et al., 2012). Studies at higher field strength, typically 3T and based on smaller samples, are now emerging (e.g., Sullivan et al., 2011). Recognizing the worth to longitudinal studies of merging data collected at different field strengths, a growing number of studies have attempted to combine data across MRI systems, typically 1.5T and 3T field strengths (Goodro et al., 2011; Han et al., 2006; Jovicich et al., 2009; Keihaninejad et al., 2010). To do so requires adjustment to minimize regional susceptibility to field effects that differentially influence tissue signal and border conspicuity (e.g., Bammer et al., 2007; Boss et al., 2007; Fushimi et al., 2007; Stankiewicz et al., 2011; Zhu et al., 2011). Recently, we showed that application of a regression-based linear correction function derived from 3T data and applied to 1.5T data on regional brain volumes determined from our SRI24 atlas-based registration and parcellation method (Rohlfing et al., 2010) significantly improved correspondence between volumes and enabled T1-weighted MRI data at both field strengths to be combined into a single analysis (Pfefferbaum et al., 2012).

The aims of the present study were to measure longitudinal changes in regional brain volumes in terms of trajectories over the full adult to senescent age range. Given the wide age range in combining longitudinal data collected over a 1 to 8 year interval in adults whose initial MRI age varied from 20 to 85 years, our analysis used a linear mixed-effects model, designed to handle mixed cross-sectional and longitudinal data. The adult data comprised MRI collected at 1.5T and at 3T field strengths; inclusion of these two independent adult samples provided some protection against the selection-maturation interaction (cf., Schaie and Hofer, 2001). A combined segmentation and atlas-based parcellation approach (Rohlfing et al., 2010) using a sequential registration approach preferable for longitudinal analysis (Sullivan et al., 2011) was used for MRI quantification, thereby enabling direct comparison of trajectory differences across different brain tissue types, structures, and regions. Inclusion of men and women also allowed testing of potential sex differences in these brain regional trajectories of volume growth and decline. To test whether and how the addition of adolescent developmental data modified the adult trajectories of regional volume changes, we conducted another set of trajectory analyses based on the adult MRI data plus adolescent MRI data collected on a 3T system from our previous study (Sullivan et al., 2011).

## Methods

### Subjects

The data reported herein were drawn from ongoing longitudinal studies of brain structure in alcoholism, HIV infection, and normal aging. The subjects in the current analysis were included because they had at least two MRIs at the same field strength and were deemed normal controls after thorough psychiatric and medical interview, as previously described

(e.g., Pfefferbaum et al., 2012; Pfefferbaum et al., 2007; Pfefferbaum et al., 2006; Rosenbloom et al., 2007; Sullivan et al., 2011). In short, clinical psychologists and research nurses administered the Structured Clinical Interview for DSM-IV (First et al., 1998) to confirm that prospective controls did not meet DSM-IV criteria for any Axis I disorder. Quantity of lifetime alcohol consumption and date of last drink were obtained by interview (Pfefferbaum et al., 1992; Skinner, 1982; Skinner and Sheu, 1982). All participants were screened by medical history questionnaire for chronic conditions that might affect brain structure, including uncontrolled hypertension and diabetes at study entry. Blood pressure recordings were also obtained from a subgroup of participants and did not identify any subject as having hypertension on the day of testing. In retrospective review, one participant was being treated with oral hypoglycemic medication for type II diabetes at study entry. All subjects had provided written informed consent or assent, depending on age, to participate in these studies, which were approved by the Institutional Review Boards of Stanford University and SRI International.

**Adult group**—Healthy adults with two or more 3T MRI data sets included 41 men, age 22 to 80 years at initial MRI, and 41 women, age 20 to 85 years at initial MRI. An additional 14 men and 26 women, all serving as control adults in ongoing studies, had undergone two to four MRIs at 1.5T field strength; their average age at first MRI was  $49.3 \pm 14.1$  years (range=20 to 72 years) for a total adult sample of 122 (55 men and 67 women). The mean  $\pm$ SD age and range at each MRI at each field strength is presented in Table 1.

Men and women were of similar education and socioeconomic status. Most were right-handed, had above average estimated intelligence, and were relatively low consumers of alcohol (Table 1). Most participants, and nearly all age 40 or older (35/36 men and 36/43 women), completed the Dementia Rating Scale (DRS) (Mattis, 2004) at one or more MRI sessions and achieved scores ranging between 132 and 144 (dementia cut-off = 124). The 8 subjects without a DRS were the following: 41 and 57 year-old women, both scientists in our laboratory; a 68 year old woman who achieved a score of 30 out of 30 on the Mini-Mental State Examination (MMSE) (Folstein et al., 1975); a 79 year old woman who achieved a 29 on the MMSE; a 66 year old man, laboratory personnel; and 3 women who performed in the normal range on a variety of other cognitive tests.

**Adolescent group**—Data for all but one adolescent boy were presented in Sullivan et al. (Sullivan et al., 2011) and were included here to extend the age range and MRI per subject of available longitudinal 3T MRI data. The current data set with two MRIs included 17 boys and 12 girls, age 10 to 14 years; 12 boys and 6 girls had three MRIs, data not previously published (Table 1). As previously described (Sullivan et al., 2011), at their initial and follow-up visits, parents and their children were interviewed by a research psychologist or other trained researcher using a structured interview (Kiddie Schedule for Affective Disorders, K-SADS) to assess current and lifetime history of psychiatric disorders (Kaufman et al., 1997). Using the probe questions of K-SADS-PL, the interviewer questioned each participant about age at first regular use of alcohol or drug and recency and frequency of use for each substance. No participant endorsed regular use of alcohol or any substance at baseline or follow-up. One parent of each child was also interviewed at each session and confirmed, without knowledge of the child's report, a negative history of regular alcohol and drug use. No further information on alcohol or drug misuse was obtained because there were no endorsements of gate (i.e., probe) questions. Other exclusionary criteria were history of loss of consciousness > 30 minutes or central nervous system diseases. Parents provided information to determine socioeconomic status (Hollingshead, 1975). Intelligence quotient (IQ) of each adolescent was measured with the Peabody Picture Vocabulary Test (Dunn and Dunn, 1997).

## MRI acquisition

**1.5T acquisition**—This set of MRI data was collected on a GE 1.5T Signa Twin whole-body system with a quadrature head coil (General Electric Healthcare, Waukesha, WI). Two coronal structural sequences were used for the analysis: a Spoiled Gradient Recalled (SPGR) echo sequence (TR=25 ms, TE=5 ms, flip angle=30, matrix=256×192, thick=2 mm, skip=0 mm, 94 slices) and a dual-echo fast spin echo (FSE) sequence (TR=7500 ms, TE1/2=13.5/108.3 ms, matrix = 256×192, thick=4 mm, skip=0 mm, 47 slices).

**3T acquisition**—This set of MR data was collected on a GE 3T Signa whole-body system with an 8-channel phased-array head coil. Data were derived from T1-weighted Inversion-Recovery Prepared SPGR images (TR=7 ms, TE=2.2 ms, TI=300 ms, matrix = 256×256, thick=1.25 mm, skip=0 mm, 124 slices) and dual-echo FSE images (TR=8583 ms, TE1/2=13.5/108.3 ms, matrix = 256×192, thick=2.5 mm, skip=0 mm, 62 slices).

## SRI24 atlas-based parcellation

For both 1.5T and 3T data, all acquired structural images were first corrected for intensity inhomogeneity by applying a second-order polynomial multiplicative bias field computed via entropy minimization (Likar et al., 2001). The late-echo FSE image was corrected using the bias field computed from the corresponding early-echo image to maintain the ratio of early- and late-echo values at each pixel, which keeps quantities derived from this ratio (e.g., T2) invariant. For each subject and each session, the bias-corrected early-echo FSE image was then registered to the bias-corrected SPGR image using intensity-based nonrigid image registration (Rohlfing and Maurer, 2003) (<http://nitrc.org/projects/cmtk>). The SPGR, early-echo FSE, and late-echo FSE images were each skull stripped using FSL's Brain Extraction Tool, BET (Smith, 2002). The early-echo and late-echo brain masks were reformatted into SPGR image space and combined with the SPGR-derived brain mask via label voting (Rohlfing and Maurer, 2005) to form the final SPGR brain mask.

The SRI24 atlas (Rohlfing et al., 2010) (<http://nitrc.org/projects/sri24>) was used as the template for parcellating all subject brain images into regional volumes for region-of-interest-based analysis. The SRI24 atlas was created from multi-spectral images of 24 subjects, all aligned via template-free groupwise nonrigid image registration. Structural parcellation maps were either transferred from other atlases (e.g., Colin27) via nonrigid registration and manually corrected, or outlined directly in the atlas, which is possible due to the clear definition of anatomical structures in the SRI24 template image as a result of the nonrigid atlas construction procedure. For a complete description of the atlas construction and its validation, the interested reader is referred to the published description of the atlas (Rohlfing et al., 2010).

For each subject, the baseline skull-stripped SPGR images were registered to the SPGR channel of the SRI24 atlas (Rohlfing et al., 2010) via nonrigid image registration (Rohlfing and Maurer, 2003). Cortical and subcortical parcellation maps for all subjects at baseline MRI were obtained by reformatting label maps defined in SRI24 space directly into SPGR image spaces using the subject-to-atlas coordinate transformations. Each follow-up MRI was nonrigidly registered to the baseline MRI for the same subject, and label maps were reformatted via concatenation of the follow-up-to-baseline transformation with the baseline-to-atlas transformation, thus producing longitudinally-consistent parcellations (Sullivan et al., 2011).

All bias-corrected and skull-stripped SPGR images were segmented into three tissue compartments (gray matter, white matter, CSF) using FSL's FAST tool (Zhang et al., 2001). As tissue priors to both initialize and guide the classification, we used the tissue probability

maps provided with the SRI24 atlas, reformatted into subject SPGR space via the same transformations described above for the atlas-based parcellation.

**SRI24 regression-based correction function (RCF)**—To compensate for across field-strength measurement discrepancies, we applied our previously derived linear regression-based correction function (RCF) for each region (Pfefferbaum et al., 2012). For each of the 23 regional volumes, the linear fit of 3T on 1.5T volume was computed and the slope and intercept were used to transform 1.5T volumes.

$$\text{Volume}_{3T_{\text{RCF}}} = (\text{Volume}_{3T} - \text{intercept}) / \text{slope}$$

### Regions of interest

The SRI24 analysis used 23 regions of interest (Figure 1), including cortical, allocortical, and subcortical gray matter regions, white matter structures, and CSF-filled spaces, as described in our prior work (Pfefferbaum et al., 2011; Pfefferbaum et al., 2006). For each subject and MRI session, gray matter volume was computed for each cortical and allocortical region, and tissue volume (gray plus white matter) was computed for each subcortical region. Also measured were CSF-filled volumes of the lateral ventricles, third ventricle, and Sylvian fissures as well as supratentorial volume.

### Statistical analysis

The first, and larger, set of analyses was based on the adult data only; the second set of analyses combined the adolescent and adult data to test the influence of adolescent brain development on regional brain volume trajectories and trajectory modeling.

Trajectories of individual subjects were calculated using a linear mixed-effects (lme) model implemented in the statistical package, R [<http://www.r-project.org/>], and based on the approach described by Laird and Ware (Laird and Ware, 1982). The lme model also allowed for testing of nested random effects; for the current analysis, the effects of age and MRI field strength were tested first and then the effects of age and sex were tested. To describe the effects of age, linear and higher-order functions (age+age<sup>2</sup> [quadratic], and age+age<sup>2</sup>+age<sup>3</sup> [cubic]) were entered to identify the best overall fit of the trajectories of each regional brain volume. In all analyses if the age<sup>3</sup> term was significant (p<.05), the cubic model was accepted. If the age<sup>3</sup> term was not significant, the age<sup>2</sup> term was similarly tested and the quadratic model accepted if significant. If the age<sup>2</sup> term was not significant, the linear model was accepted. To examine longitudinal trajectories of volume change independent of age at data acquisition, we computed the trajectory slopes of each subject for each brain region with the subject's age at acquisition entered into the model as the deviation from the mean age of the multiple MRIs available for each individual subject, which we refer to as "agecentered" (Rogosa et al., 1982). Further, a general linear model (glm) tested cross-sectional differences in regional volumes between men and women as a function of age using only the data from the initial observation, as would be the case in a simple single observation cross-sectional study. Finally, for the adult-only analysis, we used the lme model to test for age-by-individual trajectory-by-sex interactions for each regional volume. Only the last set of lme analyses that we present combined the adolescent and adult MRI data.

## Results

### Combining 1.5T vs. 3T MRI data

As noted above, to combine the data across field strengths, each regional volume at 1.5T was transformed using the regression-based correction factor (RCF) (Pfefferbaum et al., 2012). Following application of this procedure, a simple linear regression of each regional volume on supratentorial volume (SVOL) provided headsize-residualized values for each subject. Next, an lme analysis was conducted using age and field strength as predictors for each SVOL-corrected regional volume on the combined 1.5T and 3T data to test for age-by-field strength interactions. Of the 23 regional volumes, only one measure had a field strength-by-age interaction ( $t(195)=1.9848$ ,  $p=.0380$ ), which did not survive correction for multiple comparisons (family-wise Bonferroni correction for 23 regions with  $\alpha = .05$  required  $p < .002$ ). Thus, all subsequent analyses on the adult group used the combined 1.5T and 3T data, comprising 122 subjects.

### Supratentorial volume (SVOL) sex differences

For all 23 regions, men had larger age-residualized volumes than women ( $t(120)=2.370$  to  $8.247$ ,  $p=.0194$  to  $<.00001$ ). Given the known difference between men and women in intracranial volumes, an analysis examined sex differences in regional volumes (across all observations at all times) before and after SVOL correction after controlling for age using a glm. First, we tested the homogeneity-of-slopes assumption; no region met correction for multiple comparisons with either Bonferroni correction or the false discovery rate (FDR) approach. After SVOL correction, sex differences (men > women) remained for three regions, precentral cortex ( $p=.022$ ), putamen ( $p=.0118$ ), and pallidum ( $p=.0373$ ), which did not survive correction for multiple comparisons, and were small (approximately  $\pm 0.2$  SD). Thus, all subsequent analyses were conducted with SVOL-corrected data.

### Effect of age on rate of regional volume change

Lme analyses used age as the predictor for each SVOL-corrected regional volume across all subjects. Of the 23 regions, 4 were best fit with a linear model, 10 with a quadratic model, and 9 with a cubic model (Table 2, Figure 2 black regression lines). The fit of each of the three CSF measures indicated accelerated increases in volume with increasing age (quadratic or cubic fit). All but two tissue measures (caudate and corpus callosum) decreased in volume with age (linear, quadratic, or cubic fit).

### Mean volume and individual longitudinal trajectories of change with aging

Our study design combined longitudinal data collected over a ~1 to 8 year interval in adults whose initial MRI age varied from 20 to 85 years. Thus, the results in Table 2 could be due to cross-sectional differences across individuals, individual trajectories, or a combination of both factors. To examine individual longitudinal trajectories of volume change independent of age at data acquisition, we computed the trajectory slopes of each subject for each brain region with age centered on the mean age of the multiple MRIs available for each individual subject. From this analysis, we ascertained the average volume across ages and individual trajectories independent of age. To correct for multiple comparisons, we used FDR, with  $\alpha=.05$ . Volumes of the three CSF regions increased across subjects with mean age, and volumes of all tissue regions except the caudate, amygdala, and corpus callosum decreased with mean age. Age-by-volume trajectory interactions were identified in 17 regional changes, consistent with the quadratic or cubic fit noted in the above analysis conducted without centering age (Table 3).

### Effect of age and sex on rate of regional volume change

Next, lme analyses with age as the predictor of each regional volume were conducted separately for men and women (Figure 2 regression lines, blue for men and red for women). In general, as with the combined data, ventricular and sulcal volumes increased and tissue volumes decreased with aging for each sex (Table 2). As is evident from the figures, regions suggesting age-by-sex interactions were the lateral ventricles, Sylvian fissure, hippocampus, and corpus callosum.

### Sex differences in mean volume and individual longitudinal trajectories of change with aging

To test whether sex and age interacted, as suggested in Figure 2, an lme analysis used 3 factors (mean age by centered age-by-centered age by sex) as predictors of regional volume:

```
[result=lme (volume~agemean*agecentered+agecentered*sex, random=~1|subject)]
```

Results of interest were the effects of sex (regardless of age) and the interaction of centered age by sex (Table 4). None of the sex effects on regional tissue volume met FDR-corrected significance thresholds, a result consistent with the adequacy of the SVOL correction. By contrast, for the three CSF measures, the volumes of the men had steeper trajectories than those of the women, especially after age 60 years. The volumes of the putamen and pallidum also survived FDR correction, but the sex-by-volume trajectory interactions could be explained by the fact that the fits for the men and women crossed each other (Figure 2d). What appeared to be sex-by-trajectory interactions for the hippocampus and corpus callosum in Figure 2 were not supported by individual-trajectory lme analysis.

### Sex differences in trajectories of regional brain systems

We conducted a series of ANOVAs to test for sex differences in age-independent individual trajectories of each of five, anatomically-related categories of regional brain volume. Descriptive statistics (Figure 3 and Table 5), ANOVA results, and followup Scheffé test results appear in Table 5.

For CSF measures, a 2 group (men, women)-by-3 CSF region ANOVA yielded significant effects of sex and region but not an interaction. In both groups the lateral ventricles expanded faster than the Sylvian fissures, which in turn expanded faster than the third ventricle.

The neocortical tissue regions did not show a sex effect or sex-by-region interaction but did show a region effect. For men and women, the lateral and medial frontal cortices lost volume faster than the calcarine cortex.

The allocortical tissue regions showed a modest sex effect, large regional effect, but no interaction. For the men and the women, volume decline was faster in the anterior than posterior cingulate cortex; for the women, the volume decline of the precuneus was also faster than that of the posterior cingulate cortex.

The subcortical tissue structures had neither a sex effect nor sex-by-region interaction, although the region effect was significant. Followup Scheffé tests, however, indicated only that volume decline of the hippocampus was greater than that of the thalamus in men.

For the white matter tissue measures, a sex-by-region effect was described by a volume decline in centrum semiovale and a volume increase in the corpus callosum in the men. The women did not exhibit detectable volume shrinkage in these white matter structures.

### Sex differences in individual trajectory slopes over age

We next tested the adult sample for three-way interactions in those regions that had shown a significant age effect. A model for determining whether there were sex differences in how individual trajectory slopes change over age entailed entering for each observation for each individual as predictors of the volume of a region 1) an individual's average age across observations ("agemean"), 2) an individual trajectory term (the deviation from the individual's age mean at each observation, "agecentered"), and 3) sex. Significant agemean-by-agecentered-by-sex interactions for volumes of the lateral ventricles and Sylvian fissures (older men increasing more rapidly than older women) and for centrum semiovale volume, which exhibited some minimal growth in the 20 to 40 year age range and more rapid decline in the later years for the men. Additionally, more rapid decline was seen in men relative to women in the later years in the anterior cingulate, parietal, and precentral cortices and the thalamus ( $p = .0156$  to  $.00019$ , FDR-corrected).

### Cross-sectional vs. longitudinal measurement of age-related brain volumes

To emphasize the value of the lme trajectory model using longitudinal data, a similar analysis used only initial observations in a cross-sectional glm analysis of age-related differences in regional volumes. The glm analyses yielded a similar pattern of age differences as observed with the lme conducted on longitudinal data for CSF volumes, which were better fit with a polynomial than linear model. Principal differences between cross-sectional and longitudinal results affected the cortical measures, which were better fit by a quadratic or cubic function with longitudinal data but by a linear function with cross-sectional data (Table 6).

A glm analysis of the cross-sectional data with the linear, quadratic, or cubic age function and sex as predictors of each regional volume was conducted to test for age-by-sex interactions. Whereas the lme individual longitudinal trajectory analysis identified 5 regions exhibiting sex differences meeting FDR correction, none of the cross-sectional (glm) comparisons identified any significant age-by-sex interactions (Table 6).

### Longitudinal measurement of brain volumes in adolescents and adults

Having described regional brain volume trajectories across the adult age span, we introduced our previously reported volume measures obtained in young adolescents, age 10 to 13 at study entry, who had undergone the same MRI protocol on the same 3T system (Sullivan et al., 2011) used in the 3T adult sample. Inclusion of the adolescent data allowed combined modeling of brain changes that might reflect both developmental and senescent changes. Accordingly, lme analysis of the combined adolescent and adult group yielded similar fits with evidence of growth in the centrum semiovale and rapid volume regression in several cortical regions (e.g., frontal, parietal, temporal, and precuneus) from adolescence to early adulthood (Figure 4 and Table 7).

## Discussion

Longitudinal tracking of volume change in brain structures with advancing age revealed several different patterns of trajectories related to region, tissue type, rate of change, and sex. The corpus callosum was the only structure not showing a consistent volume change with age. CSF volume trajectories all showed accelerated increases with age that were best fit by quadratic models for the third ventricle and Sylvian fissures and by a cubic model for the lateral ventricles. Declines in tissue volume of the precentral and postcentral cortices and putamen were best described by linear models; thus, although these structures lost volume with aging, there was no evidence of accelerated decline in older relative to younger individuals. In contrast to these linearly declining volumes, trajectories of the temporal,

calcarine, and occipital cortices and four subcortical structures (thalamus, caudate, pallidum, and amygdala) were best modeled by quadratic fits, indicative of accelerated changes in older age, notable after age 60 years, and present in men and women.

Regional volume changes best described by cubic functions were the lateral and medial frontal, parietal, anterior and posterior cingulate cortices, insula, and precuneus. The double inflection suggested two points of accelerated change, the first near age 30 years and the second after age 60 years. This pattern is consistent with a large postmortem study, reporting greater gray matter than white matter shrinkage from age 20 to 50 years, followed by greater white matter shrinkage in very old age (Miller et al., 1980). The older-age trajectory inflections were salient for the lateral ventricles and hippocampus. Trajectories of the hippocampus showed accelerating volume decline after age 60 years similar to that noted in a longitudinal MRI analysis of 434 healthy individuals, age 8 to 85 years (Fjell, et al., 2010). That analysis modeled the effect of the starting age on the shape of the aging trajectory. By shifting the starting point to an older age at initial analysis point, the trajectory of volume decline became steeper. Our two hippocampal aging trajectories were similar whether the starting age was 10 or 20 years and, therefore, likely provide a minimally biased representation of local volume acceleration.

Comparison of the slopes of individuals' trajectories revealed a pattern of regions especially vulnerable to aging and showing faster rates of change relative to other regions showing slower declines. The CSF volumes showed a step-wise effect in their sensitivity to aging: lateral ventricles > Sylvian fissures > third ventricle. The pattern in the cortex revealed more rapid declines with aging in the lateral and medial frontal volumes than temporal, calcarine, or occipital volumes, a pattern consistent with other cross-sectional and longitudinal reports. The allocortex showed a similar anteroposterior pattern as the neocortex, where volume decline was steeper in the anterior than posterior cingulate cortices. The most salient aging difference in subcortical structures occurred in the men, whose hippocampal aging slope was steeper than their thalamic slope. Only the white matter structural comparison, however, yielded a region-by-sex interaction, indicating that decline in volume of the centrum semiovale was faster in men than women and faster than that in the corpus callosum, which actually showed no significant decline with age in either sex. We note a potential limitation of our centrum semiovale measure. Specifically, we did not measure white matter hyperintensities (WMHIs) because we focused on SPGR results, which are not particularly sensitive to detection of WMHIs. Thus, WMHIs, indicative of compromised tissue (e.g., DeCarli et al., 2005; Raz et al., 2012; Schmidt et al., 1993), may have been included in the white matter skeleton of the centrum semiovale.

As noted by Fjell et al. (Fjell et al., 2010), description of aging effects across a large age range can be substantially influenced by the age at observation and requires appropriate statistical testing of a model that includes both secular (i.e., cohort) and individual trajectories. Our use of the model to test for interactions involving age at observation, individual trajectories, and sex demonstrated more rapid increase in lateral ventricles and Sylvian fissures and more rapid decline in the centrum semiovale in older men than women.

Although cross-sectional analysis largely comported with the longitudinal analysis in description of presumed age-related volume increases in CSF and decreases in tissue, longitudinal analysis detected regional sex differences in volume declines not detected with the cross-sectional analysis. In particular, for the three CSF measures, the volumes of the men had steeper (longitudinal) trajectories than those of the women, especially after age 60 years, patterns not detected cross-sectionally.

Our last set of analyses included longitudinal MRI data collected in young adolescents, thereby extending the age range down to 10 years. Inclusion of these data in longitudinal trajectory modeling yielded the same fits as observed in the adult-only analyses in most brain regions but refined them by providing evidence of development as well as senescent change in other regions. Specifically, seven regional trajectories were better fit with a higher-order function when the adolescent data were added to the adult data, including four posterior cortical volumes (postcentral, temporal, calcarine, and occipital cortices), two subcortical volumes (thalamus and putamen), and the corpus callosum. Considering the patterns of all 23 regions, the trajectories identified continued volume growth in the centrum semiovale concurrent with rapid volume regression in several cortical regions, notably the frontal, parietal, temporal, and precuneus, from adolescence to early adulthood. The volume growth in white matter volumes has been shown to occur with normal expansion of brain size and to be a significant determinant of ultimate intracranial volume (cf., Pfefferbaum et al., 1994), possibly reflecting increasing complexity in connectivity with functional (e.g., Vogel et al., 2010) and structural (e.g., Brain Development Cooperative Group, 2012; Giedd et al., 2010; Sowell et al., 2007) development. The white matter expansion during development, including continued myelination (Yakovlev and Lecours, 1967), occurs contemporaneously with regressive processes in the cortex, which is presumed to be undergoing pruning of neurons (Chugani et al., 1987; Feinberg, 1983; Huttenlocher, 1990; Huttenlocher et al., 1982; Johnston et al., 2009) lacking connectivity, speculatively because of lack of environmental or interoceptive need or stimulation (cf., Iglesias et al., 2005). Ideally, the gap between age 15 and 20 years should be filled for a complete model. Nonetheless, the developmental trajectories observed suggest a pattern of continuity of growth of white matter through early adulthood along with decline of cortical volume, especially in frontal regions to age 30 years, followed by a shallow slope until later adulthood, described by a second dip in cortical volume shrinkage around age 60 years (cf., Brain Development Cooperative Group, 2012; Giedd et al., 2010; Sowell et al., 2007). Perhaps these two points mark the end of developmental and start of senescent changes in brain, a depiction consistent with the pattern observed in postmortem analyses of age-related differences in brain weights and gray matter-to-white matter ratios (Dekaban and Sadowsky, 1978; Miller et al., 1980). As speculated by Raz and colleagues (Raz et al., 2005), senescent decline in brain tissue volume results from a confluence of degenerative processes, including shrinkage of neurons, arborization, processes, and intralaminar myelin, collectively considered age-related neurodegeneration and, like neurodevelopment, exhibits heterochronicity of regional brain structural loss.

Application of the regression-based correction function (RCF) to combine data across field strengths (Pfefferbaum et al., 2012) enabled inclusion of data from our 1.5T cohort and our 3T cohort. Using that approach, we showed that brain regions having the greatest correspondence between RCF-corrected data were cortical, allocortical, and subcortical structures and CSF-filled spaces. The globus pallidus showed the lowest correspondence, probably because of its high iron content and field-dependent effect on signal intensity (cf., Bartzokis et al., 2007; Haacke et al., 2005; Hallgren and Sourander, 1958; Pfefferbaum et al., 2010) and may have influenced the striatal trajectories measured in our current analysis.

Using the SRI24 atlas-based parcellation approach for quantification and our regression-based correction approach to combine data at 1.5T and 3T field strengths, only two regions had substandard ICCs of volumes across field strengths: globus pallidus (ICC corrected=.599) and the postcentral cortex (ICC corrected=.764). As previously noted (Table 1, Pfefferbaum et al., 2012), all other corrected ICCs were greater than .847 [.81 is considered “substantial” (Landis and Koch, 1977)].

Longitudinal studies with cross-sectional study entry ages spanning many decades, as conducted herein, have the benefit of tracking the trajectory of development and senescence of a given brain region for each individual separately as well as describing the trajectory of the group. Because the start points of the trajectories differ widely by age, such studies also carry a significant cross-sectional factor and the liability of cohort effects related to age at study entry, that is, the selection-maturation interaction (Nesselroade, 1986). A large-scale, retrospective postmortem study by Miller and Corsellis (Miller and Corsellis, 1977) noted significant secular effects over ~100 years in 20 to 50 year old men and women, born from the late 1800s onwards and autopsied from the early 1900s onward. Over the century, brain weights were greater in men and women, suggestive of cohort effects from environmental factors, for example, nutrition, stress, and infection. Inclusion of multiple samples with unmatched study entry ages has a potential advantage of mitigating possible cohort effects (Schaie and Hofer, 2001). To the extent that 1.5T data were typically acquired earlier in a study than 3T data because of the later introduction of the higher field strength systems to human clinical research, merging of field strength data can contribute to reduction of cohort effects.

In summary, we present a longitudinal study of regional brain volume development and regression, spanning young adolescence to older adulthood, that describes heterochronicity in trajectories by brain region and sex with statistical consideration of cross-sectional effects of age at observation.

## Acknowledgments

This work was supported by NIH grants AA017347, AA005965, AA012388, AA010723, AA017168, AG017919, EB008381. All in-house image analysis software is available from <http://nitrc.org/projects/cmtk/>. The SRI24 atlas is available from <http://nitrc.org/projects/sri24/>. The authors wish to thank David R. Rogosa, Ph.D. for invaluable instruction on interpretation of longitudinal, lme analysis and understanding of R output, and Alex McMillan, Ph.D. for helpful instruction in programming and plotting in R.

## References

- Adalsteinsson E, Sullivan EV, Kleinhans N, Spielman DM, Pfefferbaum A. Longitudinal decline of the neuronal marker N-acetyl aspartate in Alzheimer's Disease. *The Lancet*. 2000; 355:1696–1697.
- Bammer R, Hope TA, Aksoy M, Alley MT. Time-resolved 3D quantitative flow MRI of the major intracranial vessels: initial experience and comparative evaluation at 1.5T and 3.0T in combination with parallel imaging. *Magn Reson Med*. 2007; 57:127–140. [PubMed: 17195166]
- Bartzokis G, Tishler TA, Lu PH, Villablanca P, Altshuler LL, Carter M, Huang D, Edwards N, Mintz J. Brain ferritin iron may influence age- and gender-related risks of neurodegeneration. *Neurobiology of Aging*. 2007; 28:414–423. [PubMed: 16563566]
- Blanton RE, Levitt JG, Thompson PM, Narr KL, Capetillo-Cunliffe L, Nobel A, Singerman JD, McCracken JT, Toga AW. Mapping cortical asymmetry and complexity patterns in normal children. *Psychiatry Res*. 2001; 107:29–43. [PubMed: 11472862]
- Blatter DD, Bigler ED, Gale SD, Johnson SC, Anderson C, Burnett BM, Parker N, Kurth S, Horn S. Quantitative volumetric analysis of brain MRI: Normative database spanning five decades of life. *American Journal of Neuroradiology*. 1995; 16:241–245. [PubMed: 7726068]
- Boss A, Martirosian P, Klose U, Nagele T, Claussen CD, Schick F. FAIR-TrueFISP imaging of cerebral perfusion in areas of high magnetic susceptibility differences at 1.5 and 3 Tesla. *J Magn Reson Imaging*. 2007; 25:924–931. [PubMed: 17410577]
- Brain Development Cooperative Group. Total and regional brain volumes in a population-based normative sample from 4 to 18 years: the NIH MRI Study of Normal Brain Development. *Cereb Cortex*. 2012; 22:1–12. [PubMed: 21613470]
- Burgmans S, van Boxtel MP, Vuurman EF, Smeets F, Gronenschild EH, Uylings HB, Jolles J. The prevalence of cortical gray matter atrophy may be overestimated in the healthy aging brain. *Neuropsychology*. 2009; 23:541–550. [PubMed: 19702408]

- Carne RP, Vogrin S, Litewka L, Cook MJ. Cerebral cortex: an MRI-based study of volume and variance with age and sex. *J Clin Neurosci*. 2006; 13:60–72. [PubMed: 16410199]
- Chugani HT, Phelps ME, Mazziotta JC. Positron emission tomography study of human brain functional development. *Annals of Neurology*. 1987; 22:487–497. [PubMed: 3501693]
- Cook IA, Leuchter AF, Morgan ML, Dunkin JJ, Witte E, David S, Mickes L, O'Hara R, Simon S, Lufkin R, Abrams M, Rosenberg S. Longitudinal progression of subclinical structural brain disease in normal aging. *American Journal of Geriatric Psychiatry*. 2004; 12:190–200. [PubMed: 15010348]
- Courchesne E, Chisum HJ, Townsend J, Cowles A, Covington J, Egaas B, Harwood M, Hinds S, Press GA. Normal brain development and aging: quantitative analysis at in vivo MR imaging in healthy volunteers. *Radiology*. 2000; 216:672–682. [PubMed: 10966694]
- DeCarli C, Fletcher E, Ramey V, Harvey D, Jagust WJ. Anatomical mapping of white matter hyperintensities (WMH): exploring the relationships between periventricular WMH, deep WMH, and total WMH burden. *Stroke*. 2005; 36:50–55. [PubMed: 15576652]
- Dekaban A, Sadowsky D. Changes in brain weights during the span of human life: Relation of brain weights to body heights and body weights. *Annals of Neurology*. 1978; 4:345–356. [PubMed: 727739]
- Driscoll I, Davatzikos C, An Y, Wu X, Shen D, Kraut M, Resnick SM. Longitudinal pattern of regional brain volume change differentiates normal aging from MCI. *Neurology*. 2009; 72:1906–1913. [PubMed: 19487648]
- Dunn, LM.; Dunn, ES. Peabody Picture Vocabulary Test. 3. American Guidance Service; Circle Pines, MN: 1997.
- Feinberg I. Schizophrenia caused by a fault in programmed synaptic elimination during adolescence? *Journal of Psychiatric Research*. 1983; 17:319–334. [PubMed: 7187776]
- First, MB.; Spitzer, RL.; Gibbon, M.; Williams, JBW. Structured Clinical Interview for DSM-IV Axis I Disorders (SCID) Version 2.0. Biometrics Research Department. New York State Psychiatric Institute; New York, NY: 1998.
- Fjell AM, Walhovd KB, Fennema-Notestine C, McEvoy LK, Hagler DJ, Holland D, Brewer JB, Dale AM. One-year brain atrophy evident in healthy aging. *Journal of Neuroscience*. 2009a; 29:15223–15231. [PubMed: 19955375]
- Fjell AM, Walhovd KB, Westlye LT, Ostby Y, Tamnes CK, Jernigan TL, Gamst A, Dale AM. When does brain aging accelerate? Dangers of quadratic fits in cross-sectional studies. *Neuroimage*. 2010; 50:1376–1383. [PubMed: 20109562]
- Fjell AM, Westlye LT, Amlien I, Espeseth T, Reinvang I, Raz N, Agartz I, Salat DH, Greve DN, Fischl B, Dale AM, Walhovd KB. Minute effects of sex on the aging brain: a multisample magnetic resonance imaging study of healthy aging and Alzheimer's disease. *Journal of Neuroscience*. 2009b; 29:8774–8783. [PubMed: 19587284]
- Folstein MF, Folstein SE, McHugh PR. Mini-mental state: A practical method for grading the cognitive state of patients for the clinician. *Journal of Psychiatric Research*. 1975; 12:189–198. [PubMed: 1202204]
- Fushimi Y, Miki Y, Urayama S, Okada T, Mori N, Hanakawa T, Fukuyama H, Togashi K. Gray matter-white matter contrast on spin-echo T1-weighted images at 3 T and 1.5 T: a quantitative comparison study. *Eur Radiol*. 2007; 17:2921–2925. [PubMed: 17619195]
- Giedd JN, Blumenthal J, Jeffries NO, Castellanos FX, Liu H, Zijdenbos A, Paus T, Evans AC, Rapoport JL. Brain development during childhood and adolescence: a longitudinal MRI study [letter]. *Nature Neuroscience*. 1999; 2:861–863.
- Giedd JN, Snell JW, Lange N, Rajapakse JC, Casey BJ, Kozuch PL, Vaituzis AC, Vauss YC, Hamburger SD, Kaysen D, Rapoport JL. Quantitative magnetic resonance imaging of human brain development: ages 4–18. *Cerebral Cortex*. 1996; 6:551–560. [PubMed: 8670681]
- Giedd JN, Stockman M, Weddle C, Liverpool M, Alexander-Bloch A, Wallace GL, Lee NR, Lalonde F, Lenroot RK. Anatomic magnetic resonance imaging of the developing child and adolescent brain and effects of genetic variation. *Neuropsychol Rev*. 2010; 20:349–361. [PubMed: 21069466]
- Gogtay N, Giedd JN, Lusk L, Hayashi KM, Greenstein D, Vaituzis AC, Nugent TF 3rd, Herman DH, Clasen LS, Toga AW, Rapoport JL, Thompson PM. Dynamic mapping of human cortical

- development during childhood through early adulthood. *Proc Natl Acad Sci U S A*. 2004; 101:8174–8179. [PubMed: 15148381]
- Goldstein JM, Seidman LJ, Horton NJ, Makris N, Kennedy DN, Caviness VS Jr, Faraone SV, Tsuang MT. Normal sexual dimorphism of the adult human brain assessed by in vivo magnetic resonance imaging. *Cereb Cortex*. 2001; 11:490–497. [PubMed: 11375910]
- Good CD, Johnsrude IS, Ashburner J, Henson RN, Friston KJ, Frackowiak RS. A voxel-based morphometric study of ageing in 465 normal adult brains. *NeuroImage*. 2001; 14:21–36. [PubMed: 11525331]
- Goodro M, Sameti M, Patenuade B, Fein G. Age effect on subcortical structures in healthy adults. *Psychiatry Research: Neuroimaging*. 2011 in press.
- Haacke EM, Cheng NY, House MJ, Liu Q, Neelavalli J, Ogg RJ, Khan A, Ayaz M, Kirsch W, Obenaus A. Imaging iron stores in the brain using magnetic resonance imaging. *Magnetic Resonance Imaging*. 2005; 23:1–25. [PubMed: 15733784]
- Hallgren B, Sourander P. The effect of age on the non-haemin iron in the human brain. *J Neurochem*. 1958; 3:41–51. [PubMed: 13611557]
- Han X, Jovicich J, Salat D, van der Kouwe A, Quinn B, Czanner S, Busa E, Pacheco J, Albert M, Killiany R, Maguire P, Rosas D, Makris N, Dale A, Dickerson B, Fischl B. Reliability of MRI-derived measurements of human cerebral cortical thickness: the effects of field strength, scanner upgrade and manufacturer. *Neuroimage*. 2006; 32:180–194. [PubMed: 16651008]
- Hollingshead, A. Four-Factor Index of Social Status. Yale University, Department of Sociology; New Haven, CT: 1975.
- Huttenlocher PR. Morphometric study of human cerebral cortex development. *Neuropsychologia*. 1990; 28:517–527. [PubMed: 2203993]
- Huttenlocher PR, de Courten C, Garey LJ, van Der Loos H. Synaptogenesis in human visual cortex: Evidence for synapse elimination during normal development. *Neuroscience Letters*. 1982; 33:247–252. [PubMed: 7162689]
- Iglesias J, Eriksson J, Grize F, Tomassini M, Villa AE. Dynamics of pruning in simulated large-scale spiking neural networks. *Biosystems*. 2005; 79:11–20. [PubMed: 15649585]
- Jack CR Jr, Petersen RC, Xu Y, O'Brien PC, Smith GE, Ivnik RJ, Boeve BF, Tangalos EG, Kokmen E. Rates of hippocampal atrophy correlate with change in clinical status in aging and AD. *Neurology*. 2000; 55:484–489. [PubMed: 10953178]
- Jernigan TL, Archibald SL, Fennema-Notestine C, Gamst AC, Stout JC, Bonner J, Hesselink JR. Effects of age on tissues and regions of the cerebrum and cerebellum. *Neurobiology of Aging*. 2001; 22:581–594. [PubMed: 11445259]
- Johnston MV, Ishida A, Ishida WN, Matsushita HB, Nishimura A, Tsuji M. Plasticity and injury in the developing brain. *Brain Dev*. 2009; 31:1–10. [PubMed: 18490122]
- Jovicich J, Czanner S, Han X, Salat D, van der Kouwe A, Quinn B, Pacheco J, Albert M, Killiany R, Blacker D, Maguire P, Rosas D, Makris N, Gollub R, Dale A, Dickerson BC, Fischl B. MRI-derived measurements of human subcortical, ventricular and intracranial brain volumes: Reliability effects of scan sessions, acquisition sequences, data analyses, scanner upgrade, scanner vendors and field strengths. *Neuroimage*. 2009; 46:177–192. [PubMed: 19233293]
- Kaufman J, Birmaher B, Brent D, Rao U, Flynn C, Moreci P, Williamson D, Ryan N. Schedule for Affective Disorders and Schizophrenia for School-Age Children-Present and Lifetime Version (K-SADS-PL): initial reliability and validity data. *J Am Acad Child Adolesc Psychiatry*. 1997; 36:980–988. [PubMed: 9204677]
- Keihaninejad S, Heckemann RA, Fagiolo G, Symms MR, Hajnal JV, Hammers A. A robust method to estimate the intracranial volume across MRI field strengths (1.5T and 3T). *Neuroimage*. 2010; 50:1427–1437. [PubMed: 20114082]
- Laird NM, Ware JH. Random-effects models for longitudinal data. *Biometrics*. 1982; 38:963–974. [PubMed: 7168798]
- Landis JR, Koch GG. The measurement of observer agreement for categorical data. *Biometrics*. 1977; 33:159–174. [PubMed: 843571]
- Lange N, Giedd JN, Castellanos FX, Vaituzis AC, Rapoport JL. Variability of human brain structure size: Ages 4–20 years. *Psychiatry Research Neuroimaging*. 1997; 74:1–12.

- Lenroot RK, Gogtay N, Greenstein DK, Wells EM, Wallace GL, Clasen LS, Blumenthal JD, Lerch J, Zijdenbos AP, Evans AC, Thompson PM, Giedd JN. Sexual dimorphism of brain developmental trajectories during childhood and adolescence. *Neuroimage*. 2007; 36:1065–1073. [PubMed: 17513132]
- Likar B, Viergever MA, Pernus F. Retrospective correction of MR intensity inhomogeneity by information minimization. *IEEE Transactions on Medical Imaging*. 2001; 20:1398–1410.
- Lindenberger U, von Oertzen T, Ghisletta P, Hertzog C. Cross-sectional age variance extraction: what's change got to do with it? *Psychol Aging*. 2011; 26:34–47. [PubMed: 21417539]
- Lu L, Leonard C, Thompson P, Kan E, Jolley J, Welcome S, Toga A, Sowell E. Normal developmental changes in inferior frontal gray matter are associated with improvement in phonological processing: a longitudinal MRI analysis. *Cereb Cortex*. 2007; 17:1092–1099. [PubMed: 16782757]
- Luft AR, Skalej M, Schulz JB, Welte D, Kolb R, Burk K, Klockgether T, Voight K. Patterns of age-related shrinkage in cerebellum and brainstem observed in vivo using three-dimensional MRI volumetry. *Cerebral Cortex*. 1999; 9:712–721. [PubMed: 10554994]
- Marcus DS, Fotenos AF, Csernansky JG, Morris JC, Buckner RL. Open access series of imaging studies: longitudinal MRI data in nondemented and demented older adults. *Journal of Cognitive Neuroscience*. 2010; 22:2677–2684. [PubMed: 19929323]
- Mattis, S. *Dementia Rating Scale (DRS) Professional Manual*. Psychological Assessment Resources, Inc; Odessa, FL: 2004.
- Miller AKH, Alston RL, Corsellis JAN. Variations with age in the volumes of grey and white matter in the cerebral hemispheres of man: measurements with an image analyzer. *Neuropathology and Applied Neurobiology*. 1980; 6:119–132. [PubMed: 7374914]
- Miller AKH, Corsellis JAN. Evidence for secular increase in human brain weight during the past century. *Annals of Human Biology*. 1977; 4:253–257. [PubMed: 900889]
- Nesselroade JR. Selection and generalization in investigations of interrelationships among variables: Some commentary on aging research. *Educational Gerontology*. 1986; 12:395–402.
- Pfefferbaum A, Adalsteinsson E, Rohlfing T, Sullivan EV. Diffusion tensor imaging of deep gray matter brain structures: Effects of age and iron concentration. *Neurobiology of Aging*. 2010; 31:482–493. [PubMed: 18513834]
- Pfefferbaum A, Chanraud S, Pitel AL, Müller-Oehring EM, Shankaranarayanan A, Alsop D, Rohlfing T, Sullivan EV. Cerebral blood flow in posterior cortical nodes of the default mode network decreases with task engagement but remains higher than in most brain regions. *Cerebral Cortex*. 2011; 21:233–244. [PubMed: 20484322]
- Pfefferbaum A, Lim KO, Zipursky RB, Mathalon DH, Rosenbloom MJ, Lane B, Ha CN, Sullivan EV. Brain gray and white matter volume loss accelerates with aging in chronic alcoholics: A quantitative MRI study. *Alcoholism: Clinical and Experimental Research*. 1992; 16:1078–1089.
- Pfefferbaum A, Mathalon DH, Sullivan EV, Rawles JM, Zipursky RB, Lim KO. A quantitative magnetic resonance imaging study of changes in brain morphology from infancy to late adulthood. *Archives of Neurology*. 1994; 51:874–887. [PubMed: 8080387]
- Pfefferbaum A, Rohlfing T, Rosenbloom MJ, Sullivan EV. Combining atlas-based parcellation of regional brain data acquired across 1.5T and 3.0T field-strengths. *NeuroImage*. 2012; 60:940–951. [PubMed: 22297204]
- Pfefferbaum A, Rosenbloom MJ, Adalsteinsson E, Sullivan EV. Diffusion tensor imaging with quantitative fiber tracking in HIV infection and alcoholism comorbidity: Synergistic white matter damage. *Brain*. 2007; 130:48–64. [PubMed: 16959813]
- Pfefferbaum A, Rosenbloom MJ, Rohlfing T, Adalsteinsson E, Kemper CA, Deresinski S, Sullivan EV. Contribution of alcoholism to brain dysmorphology in HIV infection: Effects on the ventricles and corpus callosum. *NeuroImage*. 2006; 33:239–251. [PubMed: 16877010]
- Pfefferbaum A, Sullivan EV, Rosenbloom MJ, Mathalon DH, Lim KO. A controlled study of cortical gray matter and ventricular changes in alcoholic men over a 5-year interval. *Archives of General Psychiatry*. 1998; 55:905–912. [PubMed: 9783561]

- Rabbitt P. Between-individual variability and interpretation of associations between neurophysiological and behavioral measures in aging populations: comment on Salthouse (2011). *Psychol Bull.* 2011; 137:785–789. [PubMed: 21859178]
- Raji CA, Lopez OL, Kuller LH, Carmichael OT, Becker JT. Age, Alzheimer disease, and brain structure. *Neurology.* 2009; 73:1899–1905. [PubMed: 19846828]
- Raz N, Ghisletta P, Rodrigue KM, Kennedy KM, Lindenberger U. Trajectories of brain aging in middle-aged and older adults: regional and individual differences. *Neuroimage.* 2010; 51:501–511. [PubMed: 20298790]
- Raz N, Gunning-Dixon F, Head D, Rodrigue K, Williamson A, Acker J. Aging, sexual dimorphism, and hemispheric asymmetry of the cerebral cortex: replicability of regional differences in volume. *Neurobiology of Aging.* 2004a; 25:377–396. [PubMed: 15123343]
- Raz, N.; Kennedy, KM. A systems approach to age-related change: Neuroanatomic changes, their modifiers, and cognitive correlates. In: Jagust, WJ.; D'Esposito, M., editors. *Imaging the Aging Brain.* Oxford University Press; New York: 2009. p. 43-70.
- Raz N, Lindenberger U. Only time will tell: cross-sectional studies offer no solution to the age-brain-cognition triangle: comment on Salthouse (2011). *Psychol Bull.* 2011; 137:790–795. [PubMed: 21859179]
- Raz N, Lindenberger U, Rodrigue KM, Kennedy KM, Head D, Williamson A, Dahle C, Gerstorff D, Acker JD. Regional brain changes in aging healthy adults: General trends, individual differences, and modifiers. *Cerebral Cortex.* 2005; 15:1676–1689. [PubMed: 15703252]
- Raz N, Rodrigue KM. Differential aging of the brain: Patterns, cognitive correlates and modifiers. *Neuroscience and Biobehavioral Reviews.* 2006; 30:730–748. [PubMed: 16919333]
- Raz N, Rodrigue KM, Head D, Kennedy KM, Acker JD. Differential aging of the medial temporal lobe: a study of a five-year change. *Neurology.* 2004b; 62:433–438. [PubMed: 14872026]
- Raz N, Rodrigue KM, Kennedy KM, Head D, Gunning-Dixon F, Acker JD. Differential aging of the human striatum: longitudinal evidence. *American Journal of Neuroradiology.* 2003; 24:1849–1856. [PubMed: 14561615]
- Raz N, Yang YQ, Rodrigue KM, Kennedy KM, Lindenberger U, Ghisletta P. White matter deterioration in 15 months: latent growth curve models in healthy adults. *Neurobiol Aging.* 2012; 33:429 e421–425. [PubMed: 21194799]
- Raznahan A, Lee Y, Stidd R, Long R, Greenstein D, Clasen L, Addington A, Gogtay N, Rapoport JL, Giedd JN. Longitudinally mapping the influence of sex and androgen signaling on the dynamics of human cortical maturation in adolescence. *Proceedings of the National Academy of Sciences of the United States of America.* 2010; 107:16988–16993. [PubMed: 20841422]
- Raznahan A, Lerch JP, Lee N, Greenstein D, Wallace GL, Stockman M, Clasen L, Shaw PW, Giedd JN. Patterns of coordinated anatomical change in human cortical development: a longitudinal neuroimaging study of maturational coupling. *Neuron.* 2011a; 72:873–884. [PubMed: 22153381]
- Raznahan A, Shaw P, Lalonde F, Stockman M, Wallace GL, Greenstein D, Clasen L, Gogtay N, Giedd JN. How does your cortex grow? *Journal of Neuroscience.* 2011b; 31:7174–7177. [PubMed: 21562281]
- Reiss AL, Abrams MT, Singer HS, Ross JL, Denckla MB. Brain development, gender and IQ in children. A volumetric imaging study. *Brain.* 1996; 119:1763–1774. [PubMed: 8931596]
- Resnick SM, Pham DL, Kraut MA, Zonderman AB, Davatzikos C. Longitudinal magnetic resonance imaging studies of older adults: a shrinking brain. *Journal of Neuroscience.* 2003; 23:3295–3301. [PubMed: 12716936]
- Rodrigue KM, Raz N. Shrinkage of the entorhinal cortex over five years predicts memory performance in healthy adults. *Journal of Neuroscience.* 2004; 24:956–963. [PubMed: 14749440]
- Rogosa D, Brandt D, Zimowski M. A growth curve approach to the measurement of change. *Psychological Bulletin.* 1982; 92:727–748.
- Rohlfing T, Maurer CR. Nonrigid image registration in shared-memory multiprocessor environments with application to brains, breasts, and bees. *IEEE Transactions on Information Technology in Biomedicine.* 2003; 7:16–25. [PubMed: 12670015]
- Rohlfing T, Maurer CR. Multi-classifier framework for atlas-based image segmentation. *Pattern Recognition Letters.* 2005; 26:2070–2079.

- Rohlfing T, Zahr NM, Sullivan EV, Pfefferbaum A. The SRI24 multi-channel atlas of normal adult human brain structure. *Human Brain Mapping*. 2010; 31:798–819. [PubMed: 20017133]
- Rosenbloom MJ, Sullivan EV, Sassoon SA, O'Reilly A, Fama R, Kemper CA, Deresinski SC, Pfefferbaum A. Alcoholism, HIV infection and their comorbidity: Factors affecting self-rated health-related quality of life. *Journal of Studies on Alcohol and Drugs*. 2007; 68:115–125. [PubMed: 17149525]
- Rusinek H, De Santi S, Frid D, Tsui WH, Tarshish CY, Convit A, de Leon MJ. Regional brain atrophy rate predicts future cognitive decline: 6-year longitudinal MR imaging study of normal aging. *Radiology*. 2003; 229:691–696. [PubMed: 14657306]
- Salthouse TA. Neuroanatomical substrates of age-related cognitive decline. *Psychol Bull*. 2011; 137:753–784. [PubMed: 21463028]
- Scahill RI, Frost C, Jenkins R, Whitwell JL, Rossor MN, Fox NC. A longitudinal study of brain volume changes in normal aging using serial registered magnetic resonance imaging. *Archives of Neurology*. 2003; 60:989–994.
- Schaie, KW.; Hofer, SM. Longitudinal studies in research on aging. In: Schaie, KW.; Birren, JE., editors. *Handbook of the psychology of aging*. 5. Academic Press; San Diego: 2001. p. 53-77.
- Schmidt R, Fazekas F, Offenbacher H, Dusek T, Zach E, Reinhart B, Grieshofer P, Freidl W, Eber B, Schumacher M, Koch M, Lechner H. Neuropsychologic correlates of MRI white matter hyperintensities: A study of 150 normal volunteers. *Neurology*. 1993; 43:2490–2494. [PubMed: 8255445]
- Shaw P, Kabani NJ, Lerch JP, Eckstrand K, Lenroot R, Gogtay N, Greenstein D, Clasen L, Evans A, Rapoport JL, Giedd JN, Wise SP. Neurodevelopmental trajectories of the human cerebral cortex. *J Neurosci*. 2008; 28:3586–3594. [PubMed: 18385317]
- Skinner, HA. *Development and Validation of a Lifetime Alcohol Consumption Assessment Procedure*. Addiction Research Foundation; Toronto, Canada: 1982.
- Skinner HA, Sheu WJ. Reliability of alcohol use indices: The lifetime drinking history and the MAST. *Journal of Studies on Alcohol*. 1982; 43:1157–1170. [PubMed: 7182675]
- Smith S. Fast robust automated brain extraction. *Human Brain Mapping*. 2002; 17:143–155. [PubMed: 12391568]
- Sowell ER, Peterson BS, Kan E, Woods RP, Yoshii J, Bansal R, Xu D, Zhu H, Thompson PM, Toga AW. Sex differences in cortical thickness mapped in 176 healthy individuals between 7 and 87 years of age. *Cereb Cortex*. 2007; 17:1550–1560. [PubMed: 16945978]
- Sowell ER, Thompson PM, Leonard CM, Welcome SE, Kan E, Toga AW. Longitudinal mapping of cortical thickness and brain growth in normal children. *J Neurosci*. 2004; 24:8223–8231. [PubMed: 15385605]
- Sowell ER, Thompson PM, Rex D, Kornsand D, Tessner KD, Jernigan TL, Toga AW. Mapping sulcal pattern asymmetry and local cortical surface gray matter distribution in vivo: maturation in perisylvian cortices. *Cerebral Cortex*. 2002; 12:17–26. [PubMed: 11734529]
- Stankiewicz JM, Glanz BI, Healy BC, Arora A, Neema M, Benedict RH, Guss ZD, Tauhid S, Buckle GJ, Houtchens MK, Khoury SJ, Weiner HL, Guttmann CR, Bakshi R. Brain MRI lesion load at 1.5T and 3T versus clinical status in multiple sclerosis. *J Neuroimaging*. 2011; 21:e50–56. [PubMed: 19888926]
- Stiles J, Jernigan TL. The basics of brain development. *Neuropsychol Rev*. 2010; 20:327–348. [PubMed: 21042938]
- Sullivan EV, Marsh L, Pfefferbaum A. Preservation of hippocampal volume through adulthood in healthy men and women. *Neurobiology of Aging*. 2005; 26:1093–1098. [PubMed: 15748789]
- Sullivan EV, Pfefferbaum A, Rohlfing T, Baker FC, Padilla ML, Colrain IM. Developmental change in regional brain structure over 7 months in early adolescence: Comparison of approaches for longitudinal atlas-based parcellation. *NeuroImage*. 2011; 57:214–224. [PubMed: 21511039]
- Sullivan EV, Rohlfing T, Pfefferbaum A. Longitudinal study of callosal microstructure in the normal adult aging brain using quantitative DTI fiber tracking. *Developmental Neuropsychology*. 2010; 35:233–256. [PubMed: 20446131]
- Sullivan EV, Rosenbloom MJ, Serventi KL, Pfefferbaum A. Effects of age and sex on volumes of the thalamus, pons, and cortex. *Neurobiology of Aging*. 2004; 25:185–192. [PubMed: 14749136]

- Taki Y, Kinomura S, Sato K, Goto R, Kawashima R, Fukuda H. A longitudinal study of gray matter volume decline with age and modifying factors. *Neurobiology of Aging*. 2011a; 32:907–915. [PubMed: 19497638]
- Taki Y, Kinomura S, Sato K, Goto R, Wu K, Kawashima R, Fukuda H. Correlation between baseline regional gray matter volume and global gray matter volume decline rate. *NeuroImage*. 2011b; 54:743–749. [PubMed: 20920588]
- Tang Y, Whitman GT, Lopez I, Baloh RW. Brain volume changes on longitudinal magnetic resonance imaging in normal older people. *Journal of Neuroimaging*. 2001; 11:393–400. [PubMed: 11677879]
- Tisserand DJ, Pruessner JC, Sanz Arigita EJ, van Boxtel MP, Evans AC, Jolles J, Uylings HB. Regional frontal cortical volumes decrease differentially in aging: an MRI study to compare volumetric approaches and voxel-based morphometry. *NeuroImage*. 2002; 17:657–669. [PubMed: 12377141]
- Vogel AC, Power JD, Petersen SE, Schlaggar BL. Development of the brain's functional network architecture. *Neuropsychol Rev*. 2010; 20:362–375. [PubMed: 20976563]
- Walhovd KB, Westlye LT, Amlie I, Espeseth T, Reinvang I, Raz N, Agartz I, Salat DH, Greve DN, Fischl B, Dale AM, Fjell AM. Consistent neuroanatomical age-related volume differences across multiple samples. *Neurobiol Aging*. 2011; 32:916–932. [PubMed: 19570593]
- Weiner MW, Veitch DP, Aisen PS, Beckett LA, Cairns NJ, Green RC, Harvey D, Jack CR, Jagust W, Liu E, Morris JC, Petersen RC, Saykin AJ, Schmidt ME, Shaw L, Siuciak JA, Soares H, Toga AW, Trojanowski JQ. The Alzheimer's Disease Neuroimaging Initiative: a review of papers published since its inception. *Alzheimers Dement*. 2012; 8:S1–68. [PubMed: 22047634]
- Yakovlev, PI.; Lecours, A-R. The myelogenetic cycles of regional maturation of the brain. In: Minkowski, A., editor. *Regional Development of the Brain in Early Life*. Blackwell Scientific Publications; Oxford: 1967. p. 3-70.
- Zhang Y, Brady M, Smith S. Segmentation of brain MR images through a hidden Markov random field model and the expectation maximization algorithm. *IEEE Transactions Medical Imaging*. 2001; 20:45–57.
- Zhu YC, Dufouil C, Tzourio C, Chabriat H. Silent brain infarcts: a review of MRI diagnostic criteria. *Stroke*. 2011; 42:1140–1145. [PubMed: 21393597]

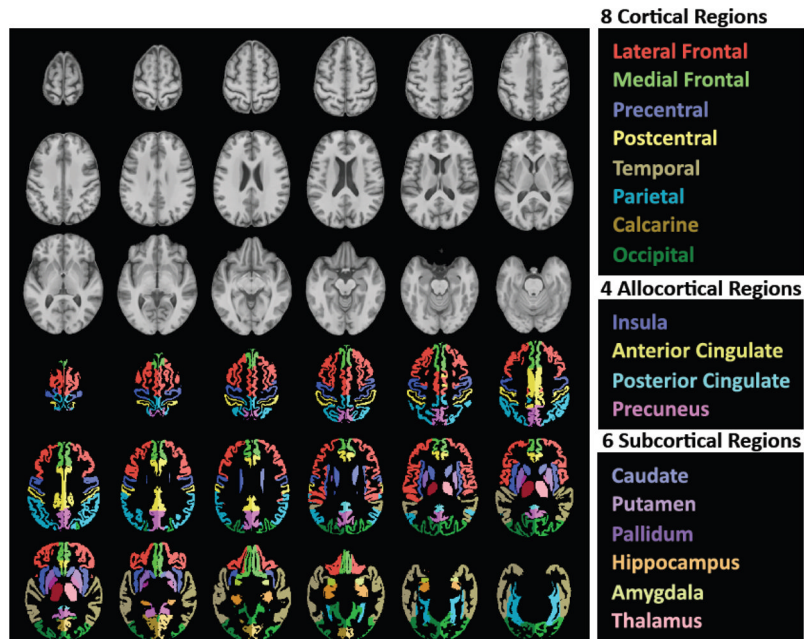


**Figure 1.**

Top three rows of gray-tone figures: Axial slices from superior to inferior (top left to bottom right) of T1-weighted SRI24 atlas template image. Bottom three rows of color figures: The same axial slices with selected, color-coded parcellated structures delineated in the SRI24 atlas.

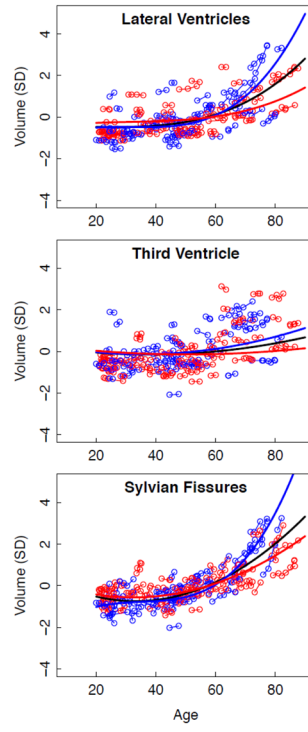


Fig. 2a

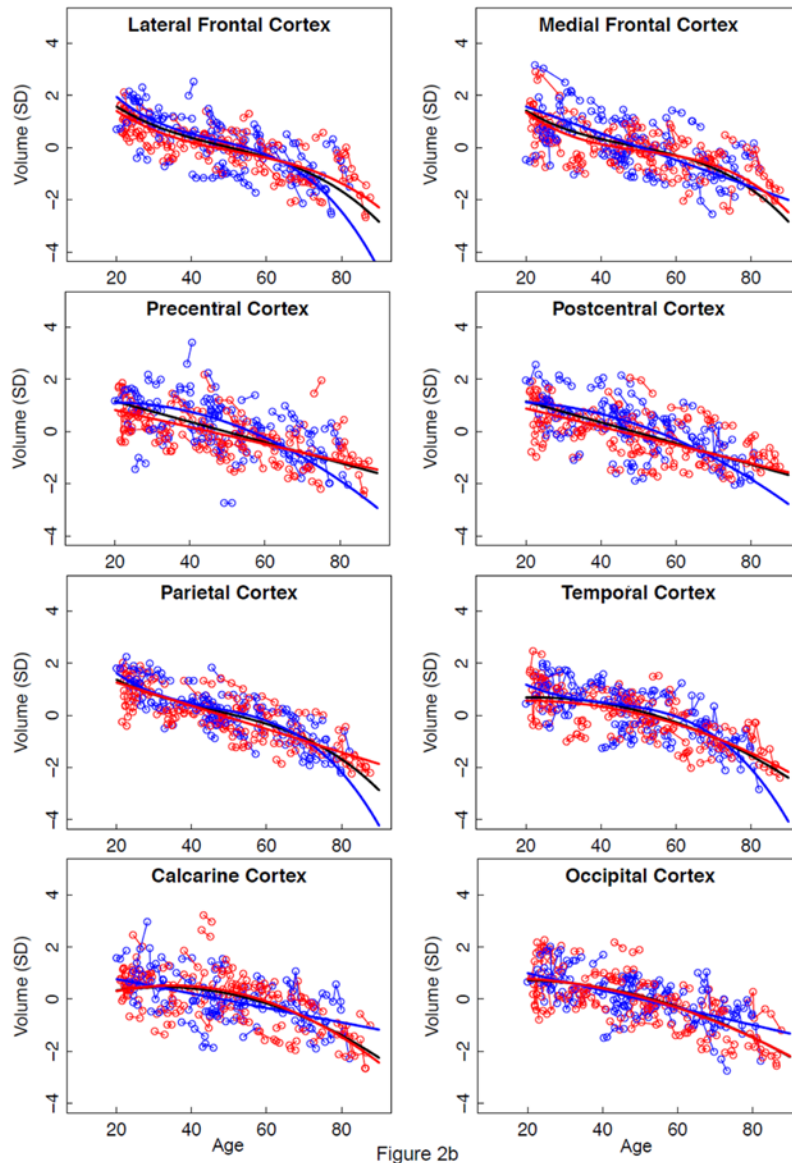


Figure 2b

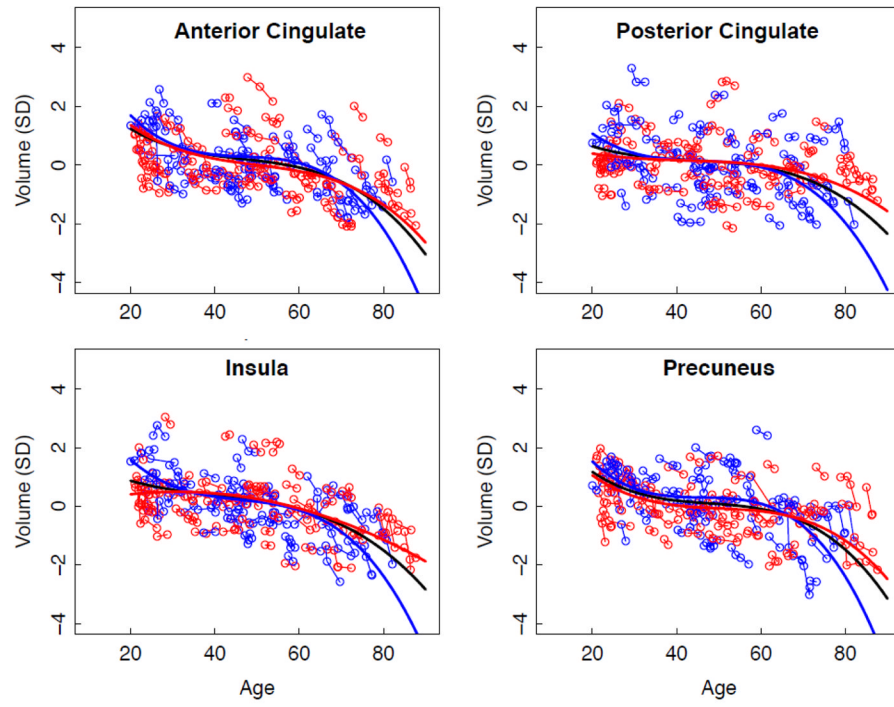


Fig. 2c

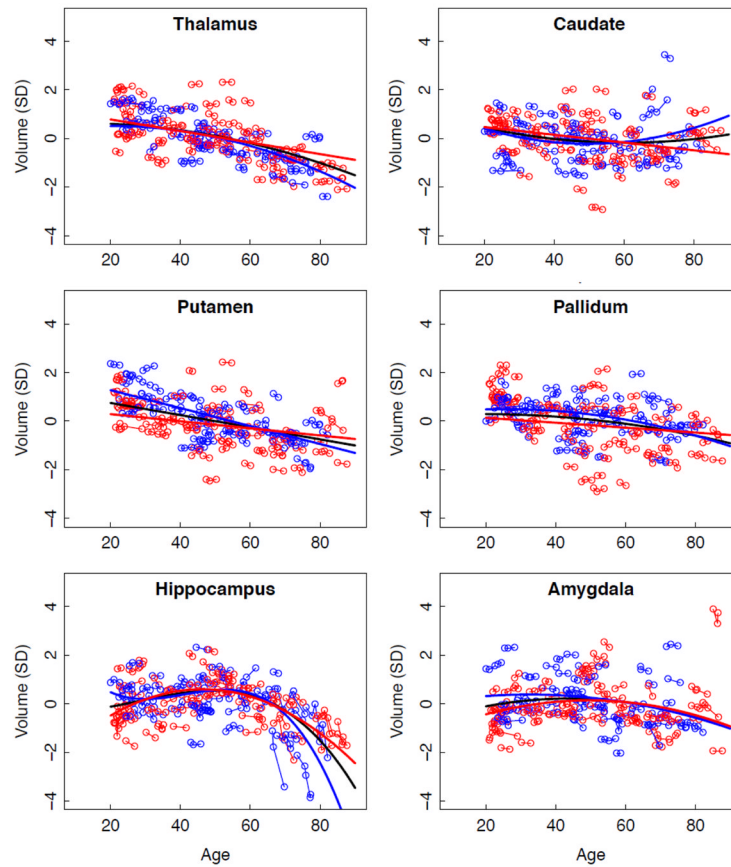


Fig. 2d

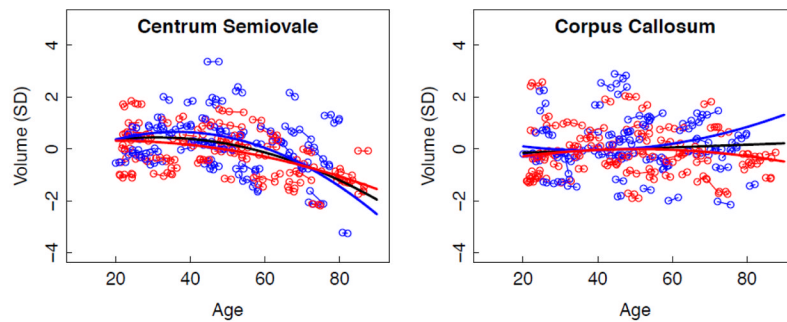
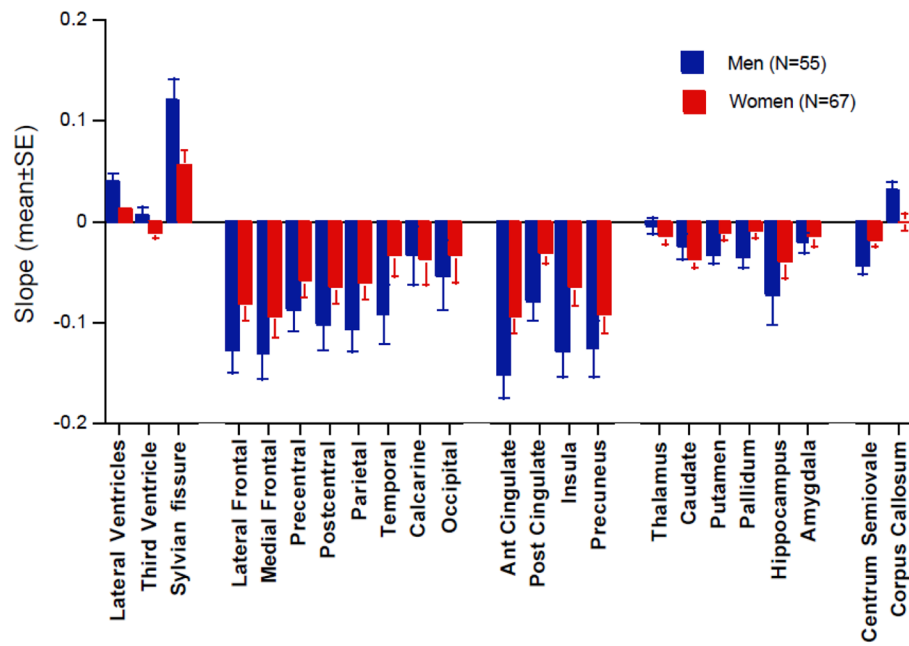


Fig. 2e

**Figure 2.**  
**a–e.** Volumes, expressed as standardized residuals (Z-score) or standard deviations (SD), after correction for supratentorial volume (SVOL) of regional brain structures of individual men (blue) and women (red) and best-fit functions over age for each sex. The black fit is the combined group, irrespective of sex.



**Figure 3.**

Mean  $\pm$  standard error (SE) of age-centered trajectory slopes of each of the 23 brain measures for the adults. Men had significantly greater slopes of the three CSF-filled structures. See Table 5 for statistical results.

\$watermark-text

\$watermark-text

\$watermark-text

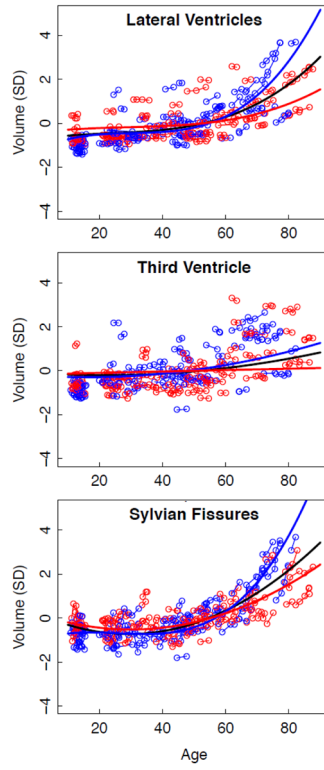


Fig. 4a

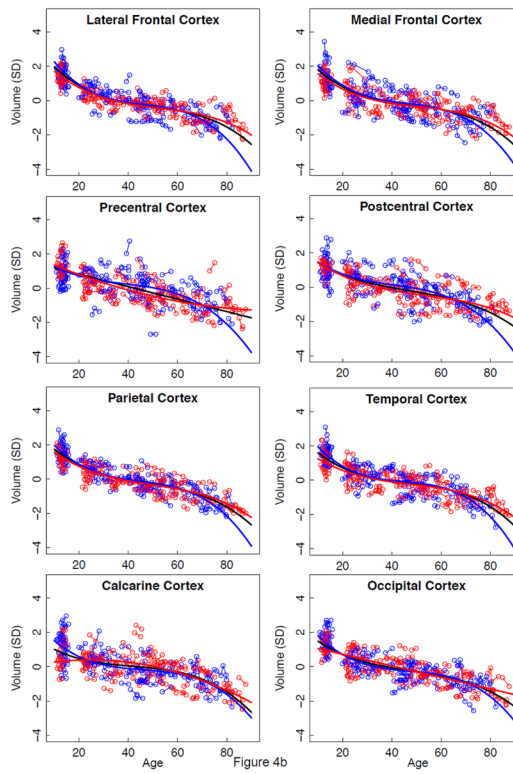


Figure 4b

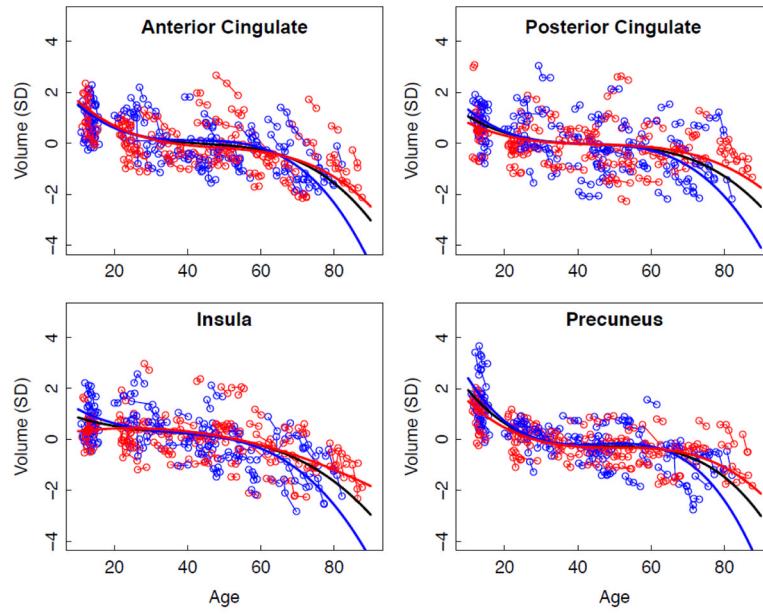


Fig. 4c

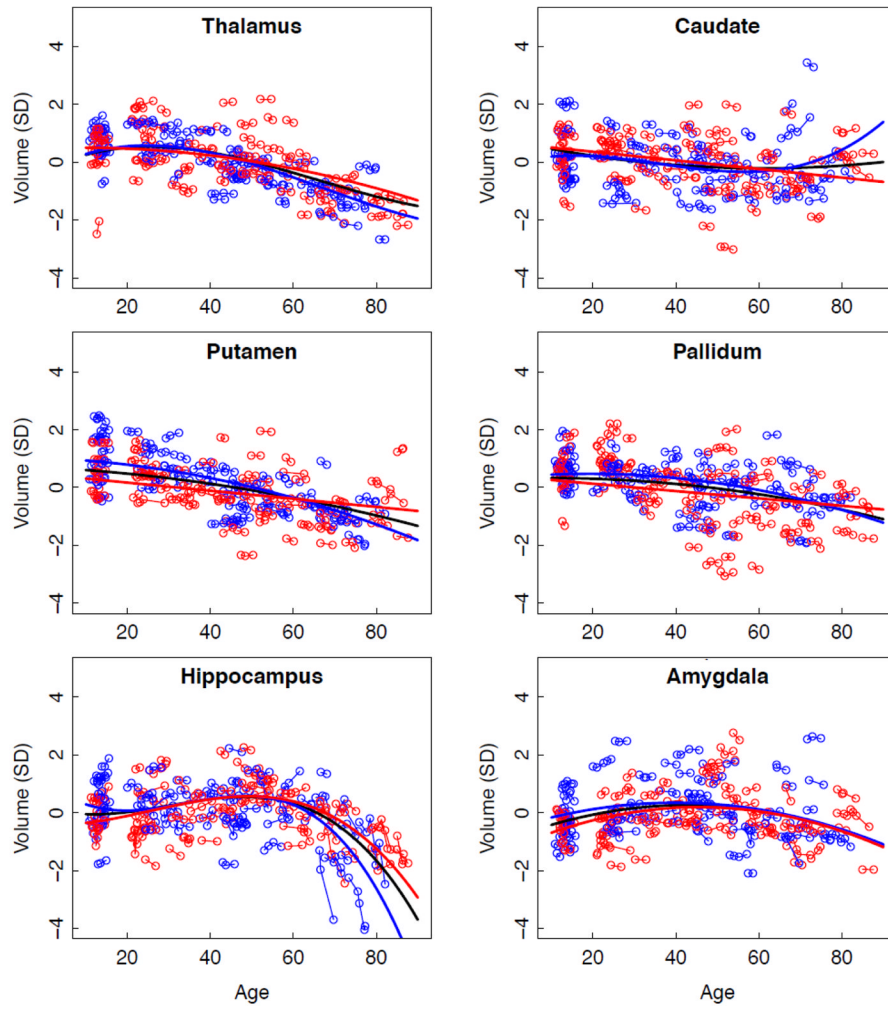


Fig. 4d

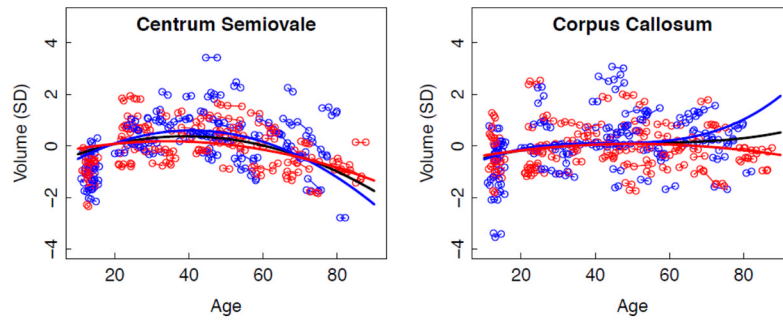


Fig. 4e

**Figure 4.** a–e. Volumes, expressed as standardized residuals (Z-score) or standard deviations (SD), after correction for supratentorial volume (SVOL) of regional brain structures of the adult plus adolescent samples, with boys and men (blue) and girls and women (red) and best-fit functions over age for each sex. The black fit is the combined group, irrespective of sex.

**Table 1**

Demographic information for men and women at initial MRI (mean±SD and N)

	3.0T		1.5T		1.5T+3.0T	
	Men	Women	Men	Women	Men	Women
<b>Age at 1st MRI</b>	mean = 47.9	45.2	43.6	52.4	46.8	48.0
	SD= 16.0	21.3	16.9	11.5	13.1	18.4
	range= 22–80	20–85	20–71	29–72	20–80	20–85
	N = 41	41	14	26	55	67
<b>Age at 2nd MRI</b>	mean= 49.6	47.0	45.1	54	48.5	49.7
	SD= 16.0	21.5	17.1	11.7	16.2	18.6
	range= 24–82	21–87	20–73	29–74	20–82	21–87
	N = 41	41	14	26	55	67
<b>Age at 3rd MRI</b>	mean = 53.6	46.8	41.8	55.8	50.7	49.3
	SD= 15.7	25.5	19.0	15.3	17.0	23.2
	range= 26–78	21–86	22–74	33–74	22–78	21–86
	N = 18	16	6	6	24	22
<b>Age at 4th MRI</b>	mean= 56.2	43.5	45.6	54.2	55.3	46.2
	SD= 18.3	26.5	–	18.3	17.7	24.4
	range= 26–79	23–83	45	54–72	26–79	23–83
	N = 10	9	1	2	11	12
<b>Age at 5th MRI</b>	mean= 67.2	50.8	–	–	67.2	50.8
	SD= 13.1	30.5			13.1	30.5
	range= 47–79	29–72			47–79	29–72
	N = 6	2			6	2
<b>Education (years)</b>	mean= 16.1	16.4	14.8	16.5	15.8	16.5
	SD= 2.3	2.2	2.5	2.5	2.4	2.3
	N = 41	41	14	26	55	67
<b>Socioeconomic Status (SES)</b>	mean= 25.3	25	34.7	22.2	27.6	24.0
	SD= 11.1	9.7	14.4	10.4	12.5	9.9
	N = 41	41	13	23	54	64
<b>Handedness</b>	mean= 20.7	21.5	23.6	19.2	21.6	20.5
	SD= 6.9	9.3	13.3	10.6	9.1	9.8

	3.0T		1.5T		1.5T + 3.0T	
	Men	Women	Men	Women	Men	Women
<b>Body Mass Index (BMI)</b>	N = 35	33	14	24	49	57
	mean = 26.0	24	26.8	23.8	26.2	23.9
	SD = 3.7	7.5	4.8	5.1	3.9	6.7
<b>Estimated IQ</b>	N = 40	41	11	22	51	63
	mean = 114.5	117	108.3	113.3	112.4	115.0
	SD = 9.5	6.8	4.6	7.1	8.6	7.1
<b>Dementia Rating Scale (DRS) Total</b>	N = 26	23	13	26	39	49
	mean = 139.8	141.0	139.8	141.8	139.8	141.4
	SD = 2.6	2.1	1.6	1.9	2.3	2
<b>Lifetime alcohol consumption (kg)</b>	N = 32	24	13	21	45	45
	mean = 54.9	15.3	111.3	141.8	67.9	14.8
	SD = 92.0	14.9	146.4	1.9	107.5	15.7
<b>Smoker</b>	N = 30	23	9	21	39	30
	yes/no	14/27	11/29	9/5	2/24	19/36

SD=standard deviation; N=number of subjects

SES: Low scores reflect higher SES

Handedness: right handedness=14-32; left handedness=50-70 (Crovitz and Zener, 1962)

Estimated IQ: mean of NART-IQ and ANART-IQ where available Peabody Picture Vocabulary Test for adolescents

**Table 2**  
Best fit tests of SVOL-corrected volume trajectories over age for all adults and for men and women separately

Region	Men + Women (N = 122)			Men (N=55)			Women (N=67)			
	t	p	FDR	best curve fit	t	p	best curve fit	t	p	best curve fit
Lateral Ventricles	2.7431	.0067	*	cubic	4.5855	.0000	cubic	3.8816	.0002	cubic
Third Ventricle	3.6671	.0003	*	quadratic	3.0743	.0028	quadratic	2.0040	.0477	quadratic
Sylvian Fissures	8.5119	.0000	*	quadratic	3.5217	.0007	cubic	5.5151	.0000	quadratic
Lateral Frontal Cortex	-2.9798	.0032	*	cubic	-2.9786	.0037	cubic	-2.6285	.0099	cubic
Medial Frontal Cortex	-3.1146	.0021	*	cubic	-7.8071	.0000	linear	-3.2953	.0014	cubic
Precentral Cortex	-9.7764	.0000	*	linear	-2.4915	.0145	quadratic	-7.0530	.0000	linear
Postcentral Cortex	-10.2411	.0000	*	linear	-2.0633	.0418	quadratic	-7.2801	.0000	linear
Parietal Cortex	-2.6816	.0080	*	cubic	-2.9171	.0044	cubic	-11.3402	.0000	linear
Temporal Cortex	-4.0235	.0001	*	quadratic	-2.1303	.0358	cubic	-2.7343	.0074	quadratic
Calcarine Cortex	-4.1049	.0001	*	quadratic	-4.6237	.0000	linear	-3.9319	.0002	quadratic
Occipital Cortex	-3.0871	.0023	*	quadratic	-6.8023	.0000	linear	-2.1498	.0340	quadratic
Anterior Cingulate Cortex	-3.5027	.0006	*	cubic	-3.5546	.0006	cubic	-3.4712	.0008	cubic
Posterior Cingulate Cortex	-3.3641	.0009	*	cubic	-3.7995	.0003	cubic	-2.1729	.0322	cubic
Insula	-2.2715	.0242	*	cubic	-3.4538	.0008	cubic	-2.9966	.0034	quadratic
Precuneus	-4.1290	.0001	*	cubic	-3.7769	.0003	cubic	-3.5054	.0007	cubic
Thalamus	-3.9032	.0001	*	quadratic	-3.8136	.0002	quadratic	-6.6825	.0000	linear
Caudate	3.3824	.0009	*†	quadratic	3.6849	.0004	quadratic	-4.0224	.0001	linear
Putamen	-8.3422	.0000	*	linear	-9.0948	.0000	linear	-3.6402	.0004	linear
Pallidum	-2.1328	.0342	*	quadratic	-2.3375	.0215	quadratic	-2.1071	.0376	linear
Hippocampus	-2.7292	.0069	*	cubic	-3.8513	.0002	cubic	-7.6729	.0000	quadratic
Amygdala	-4.5450	.0000	*	quadratic	-2.1767	.0320	quadratic	-4.0451	.0001	quadratic
Centrum Semiovale	-7.5763	.0000	*	quadratic	-6.9309	.0000	quadratic	-4.0268	.0001	quadratic
Corpus Callosum	-1.3681	.1728	*	linear	2.7776	.0066	quadratic	-2.7536	.0070	quadratic

\$watermark-text

\$watermark-text

\$watermark-text

\* FDR= false discovery rate,  $p=0.05$

\*\*<sub>f</sub> lower-order term in unexpected direction

Table 3

ANOVA results for age-centered volumes of longitudinal trajectories

Region	Volume at Mean Ages Effect			Age-by-Volume Trajectory Interaction		
	df	t	p FDR	df	t	p FDR
Lateral Ventricles	120	8.95848	.00000 *	197	9.91037	.00000 *
Third Ventricle	120	6.79041	.00000 *	197	2.87763	.00445 *
Sylvian Fissures	120	11.05846	.00000 *	197	9.04335	.00000 *
Lateral Frontal Cortex	120	-11.84789	.00000 *	197	-2.31901	.02142
Medial Frontal Cortex	120	-8.66803	.00000 *	197	-2.5453	.01168
Precentral Cortex	120	-7.01242	.00000 *	197	-1.74149	.08316
Postcentral Cortex	120	-7.49142	.00000 *	197	-2.13276	.03418
Parietal Cortex	120	-13.55924	.00000 *	197	-3.57912	.00043 *
Temporal Cortex	120	-11.04099	.00000 *	197	-4.52385	.00001 *
Calcarine Cortex	120	-7.31196	.00000 *	197	-4.41283	.00002 *
Occipital Cortex	120	-10.95272	.00000 *	197	-3.55935	.00047 *
Anterior Cingulate Cortex	120	-5.38524	.00000 *	197	-3.87876	.00014 *
Posterior Cingulate Cortex	120	-2.83808	.00533 *	197	-4.15135	.00005 *
Insula	120	-6.54018	.00000 *	197	-4.68928	.00001 *
Precuneus	120	-5.29627	.00000 *	197	-3.8016	.00019 *
Thalamus	120	-10.29237	.00000 *	197	-3.34852	.00097 *
Caudate	120	-0.69196	.49030	197	2.88059	.00441 *
Putamen	120	-7.27889	.00000 *	197	-2.29159	.02299
Pallidum	120	-5.07171	.00000 *	197	-3.02313	.00283 *
Hippocampus	120	-3.39159	.00094 *	197	-7.72059	.00000 *
Amygdala	120	-0.82663	.41009	197	-4.41392	.00002 *
Centrum Semiovale	120	-4.44389	.00002 *	197	-6.99384	.00000 *
Corpus Callosum	120	-1.02166	.30900	197	0.99337	.32175

ANOVA=analysis of variance

df=degrees of freedom

FDR= false discovery rate, p=.05

**Table 4**

Mean volume and individual longitudinal trajectories of change with aging

Region	Volume by Sex			Sex-by-Volume Trajectory Interaction		
	df	t	p	df	t	p FDR
Lateral Ventricles	119	.18681	.85213	196	4.87353	.00000 *
Third Ventricle	119	1.04153	.29974	196	2.71853	.00715 *
Sylvian Fissures	119	-.45161	.65237	196	2.77317	.00609 *
Lateral Frontal Cortex	119	1.17353	.24293	196	-1.72042	.08693
Medial Frontal Cortex	119	1.15046	.25226	196	-.53250	.59498
Precentral Cortex	119	2.13919	.03446	196	-2.27100	.02423
Postcentral Cortex	119	1.88726	.06156	196	-.91249	.36263
Parietal Cortex	119	1.04615	.29761	196	-.88131	.37923
Temporal Cortex	119	1.72495	.08713	196	-.85534	.39341
Calcarine Cortex	119	-.29213	.77069	196	.21652	.82881
Occipital Cortex	119	.51869	.60494	196	-.19775	.84345
Anterior Cingulate Cortex	119	.89011	.37520	196	-1.34662	.17966
Posterior Cingulate Cortex	119	-.14245	.88697	196	-2.31795	.02148
Insula	119	-.11253	.91060	196	-2.15853	.03210
Precuneus	119	1.10390	.27186	196	-.56495	.57275
Thalamus	119	-1.18492	.23841	196	-.28430	.77648
Caudate	119	-.62883	.53066	196	2.33919	.02033
Putamen	119	2.27087	.02495	196	-2.93261	.00376 *
Pallidum	119	2.12342	.03579	196	-3.20705	.00157 *
Hippocampus	119	.35188	.72555	196	-.96833	.33407
Amygdala	119	1.34833	.18011	196	-.81389	.41669
Centrum Semiovale	119	1.96098	.05222	196	-1.53888	.12545
Corpus Callosum	119	1.27063	.20634	196	2.13521	.03399

df=degrees of freedom

\* FDR= false discovery rate, p=.05

\$watermark-text

\$watermark-text

\$watermark-text

Table 5

Age-centered trajectories (slopes) of the 23 ROIs for men and women: Mean, SD, SE, ANOVAs, t-test p-values for sex differences and ANOVAs across ROIs within sex

ROI	Men (N = 55)			Women (N = 67)			ANOVA	t-tests: M v F		Within-Sex ANOVA across ROIs (Scheffe)
	Mean	SD	SE	Mean	SD	SE		Sex x ROI	p-value	
<b>CSF-filled Regions</b>										
Lateral Ventricles	.0397	.0658	.0089	.0133	.0319	.0039	Sex p = .0012 ROI p = .0001 Sex x ROI p = .068	.0046	LatVent>Sylvian	LatVent>Sylvian
Third Ventricle	.0071	.0080	.0080	-.0114	.0056	.0056		.0553	Sylvian>3Vent	Sylvian>3Vent
Sylvian fissure	.1201	.1606	.0217	.0560	.1136	.0139		.0113		
<b>Neocortex</b>										
Lateral Frontal	-.1255	.1720	.0232	-.0799	.1364	.0167	Sex p = .2002 ROI p = .0001 Sex x ROI p = .5623	.1046	Lat Frnt > Calc	Trend: Lat Frnt>Tmp,Calc,Occ
Medial Frontal	-.1305	.1843	.0248	-.0933	.01681	.0205		.2469	Med Frnt > Calc	Trend: Med Frnt >Tmp,Calc,Occ
Precentral	-.0864	.1603	.0216	-.0575	.1318	.0161		.2758		
Postcentral	-.1025	.1763	.0238	-.0647	.1281	.0156		.1731		
Parietal	-.1067	.1624	.0219	-.0599	.1316	.0161		.0810		
Temporal	-.0905	.2138	.0288	-.0326	.1749	.0214		.1023		
Calcarine	-.0326	.2136	.0288	-.0363	.2087	.0255		.9217		
Occipital	-.0532	.2537	.0342	-.0324	.2284	.0279		.6357		
<b>Allocortex</b>										
Anterior Cingulate Cortex	-.1503	.1835	.0247	-.0928	.1321	.0161	Sex p = .0416 ROI p = .0001 Sex x ROI p = .5907	.0469	Ant>Post Cing	Ant>Post Cing
Posterior Cingulate Cortex	-.0796	.1383	.0187	-.0304	.0864	.0106		.0180		Precun>Post Cing
Insula	-.1288	.1841	.0248	-.0639	.1626	.0199		.0410		
Precuneus	-.1254	.2075	.0280	-.0914	.1571	.0192		.3065		
<b>Subcortical Structures</b>										
Thalamus	-.0047	.0634	.0086	-.0151	.0598	.0073	Sex p = .2461 ROI p = .0032 Sex x ROI p = .183	.3545	Hipp>Thal	n.s.
Caudate	-.0247	.0863	.0116	-.0380	.0606	.0074		.3191		
Putamen	-.0332	.0571	.0077	-.0105	.0620	.0076		0.386		
Pallidum	-.0359	.0787	.0106	-.0081	.0714	.0087		.0428		
Hippocampus	-.0718	.2144	.0289	-.0385	.1351	.0165		.2989		
Amygdala	-.0211	.0786	.0106	-.0140	.0903	.0110		.6485		
<b>White Matter</b>										

ROI	Men (N = 55)			Women (N = 67)			ANOVA		t-tests: M v F		Within-Sex ANOVA across ROIs (Scheffe)	
	Mean	SD	SE	Mean	SD	SE	Sex x ROI	p-value	Men	Women		
Centrum Semiovale	-.0425	.0660	.0089	-.0185	.0536	.0066	Sex p = .6263 ROI p = .0001	.0283	Centrum >Corpus	n.s.		
Corpus Callosum	.0309	.0657	.0089	-.0002	.0670	.0082	Sex x ROI p = .0024	.0113				

Table 6

Slopes of SVOL-corrected regional volumes over age for cross-sectional data

Region	Volume over age			Volume over age and sex		
	t	p	FDR	best fit	t	p <sup>#</sup>
Lateral Ventricles	3.26864	.00141	*	quadratic	1.02289	.30849
Third Ventricle	-2.10049	.03782	*†	cubic	-.69252	.49002
Sylvian Fissures	4.50634	.00002	*	quadratic	2.12449	.03575
Lateral Frontal Cortex	-11.27923	.00000	*	linear	-1.22095	.22454
Medial Frontal Cortex	-7.91181	.00000	*	linear	-.36044	.71916
Precentral Cortex	-6.83645	.00000	*	linear	-.30637	.75986
Postcentral Cortex	-7.02428	.00000	*	linear	-1.04299	.29908
Parietal Cortex	-13.14970	.00000	*	linear	-.36241	.71770
Temporal Cortex	-10.39591	.00000	*	linear	-1.34508	.18118
Calcarine Cortex	-6.45304	.00000	*	linear	.61709	.53836
Occipital Cortex	-10.55671	.00000	*	linear	1.49778	.13686
Anterior Cingulate Cortex	-4.85214	.00000	*	linear	-.96447	.33678
Posterior Cingulate Cortex	-2.63919	.00941	*	linear	-1.19576	.23419
Insula	-5.89171	.00000	*	linear	-1.67202	.09717
Precuneus	-4.93880	.00000	*	linear	-1.19628	.23399
Thalamus	-10.07233	.00000	*	linear	-.52865	.59804
Caudate	-1.78937	.07610		linear	.74405	.45834
Putamen	2.46346	.01519	*†	quadratic	.62671	.53208
Pallidum	-5.02306	.00000	*	linear	1.73323	.08567
Hippocampus	-4.41357	.00002	*	quadratic	.69544	.48817
Amygdala	2.59266	.01073	*†	cubic	-1.14090	.25630
Centrum Semiovale	-3.42660	.00084	*	quadratic	-1.75237	.08235
Corpus Callosum	-1.15751	.24937		linear	-.46150	.64529

\* FDR= false discovery rate, p=.05

\$watermark-text

\$watermark-text

\$watermark-text

\*<sup>z</sup> lower-order term in unexpected direction

#None met FDR  $p = .05$

**Table 7**

SVOL-corrected trajectories of regional volumes over age

Region	Adolescents + Adults (N = 151)		
	t	p FDR	best fit
Lateral Ventricles	4.16071	.00004 *	cubic
Third Ventricle	3.20046	.00155 *	quadratic
Sylvian Fissures	10.84126	.00000 *	quadratic
Lateral Frontal Cortex	-6.19092	.00000 *	cubic
Medial Frontal Cortex	-5.23801	.00000 *	cubic
Precentral Cortex	-13.46334	.00000 *	linear
Postcentral Cortex	-2.70526	.00731 *	cubic
Parietal Cortex	-5.55705	.00000 *	cubic
Temporal Cortex	-5.18987	.00000 *	cubic
Calcarine Cortex	-3.41084	.00076 *	cubic
Occipital Cortex	-3.65920	.00031 *	cubic
Anterior Cingulate Cortex	-4.75743	.00000 *	cubic
Posterior Cingulate Cortex	-4.99639	.00000 *	cubic
Insula	-2.74021	.00660 *	cubic
Precuneus	-7.92646	.00000 *	cubic
Thalamus	3.18856	.00162 *	cubic
Caudate	2.81216	.00533 *	quadratic
Putamen	-2.19611	.02903 *	quadratic
Pallidum	-2.37314	.01841 *	quadratic
Hippocampus	-4.28229	.00003 *	cubic
Amygdala	-6.38594	.00000 *	quadratic
Centrum Semiovale	-11.13289	.00000 *	quadratic
Corpus Callosum	2.14031	.03333 *	cubic

\* FDR= false discovery rate, p=.05